Supplementary Information

A Comparative Photophysical Study of Structural Modifications of Thioflavin T-Inspired Fluorophores

Lisa-Maria Needham[a], Judith Weber[a,b,c], Colin M. Pearson[d], Dung T. Do[d], Felix Gorka[a], Guanpeng Lyu[a], Sarah E. Bohndiek[b], Thomas N. Snaddon[d]* and Steven F. Lee[a]*

Author Information

***** denotes joint corresponding authors

[a] Department of Chemistry, University of Cambridge, Cambridge, CB2 1EW, UK

[b] Department of Physics, University of Cambridge, Cambridge, CB3 0HE, UK

[c] Cancer Research UK Cambridge Institute, University of Cambridge, Cambridge, CB2 0RE, UK

[d] Department of Chemistry, Indiana University, Bloomington, Indiana, 47405, USA

Contents

1. Supplementary Results

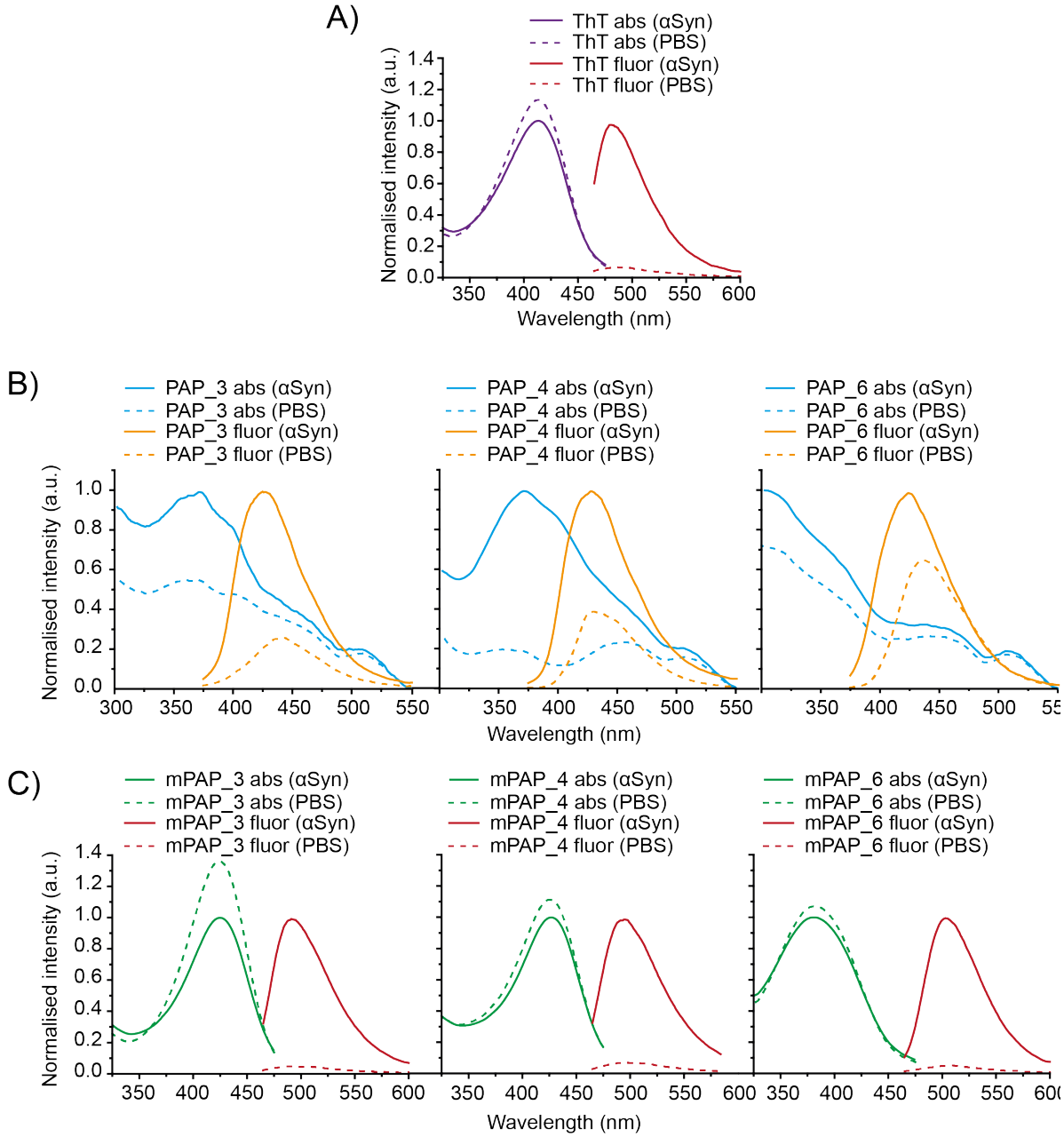

Figure S1. Bulk UV-vis absorption and emission spectra of 10 μM **A)** ThT**, B)** PAP derivatives (PAP_3 PAP_5 and PAP_6) and **C)** mPAP derivatives (mPAP_3 mPAP_5, mPAP_6) in PBS and with 2 μM recombinant αSyn aggregates (>96 hours). The spectra have been independently normalised relative to the maximum intensity of the dye in the presence of αSyn aggregates.

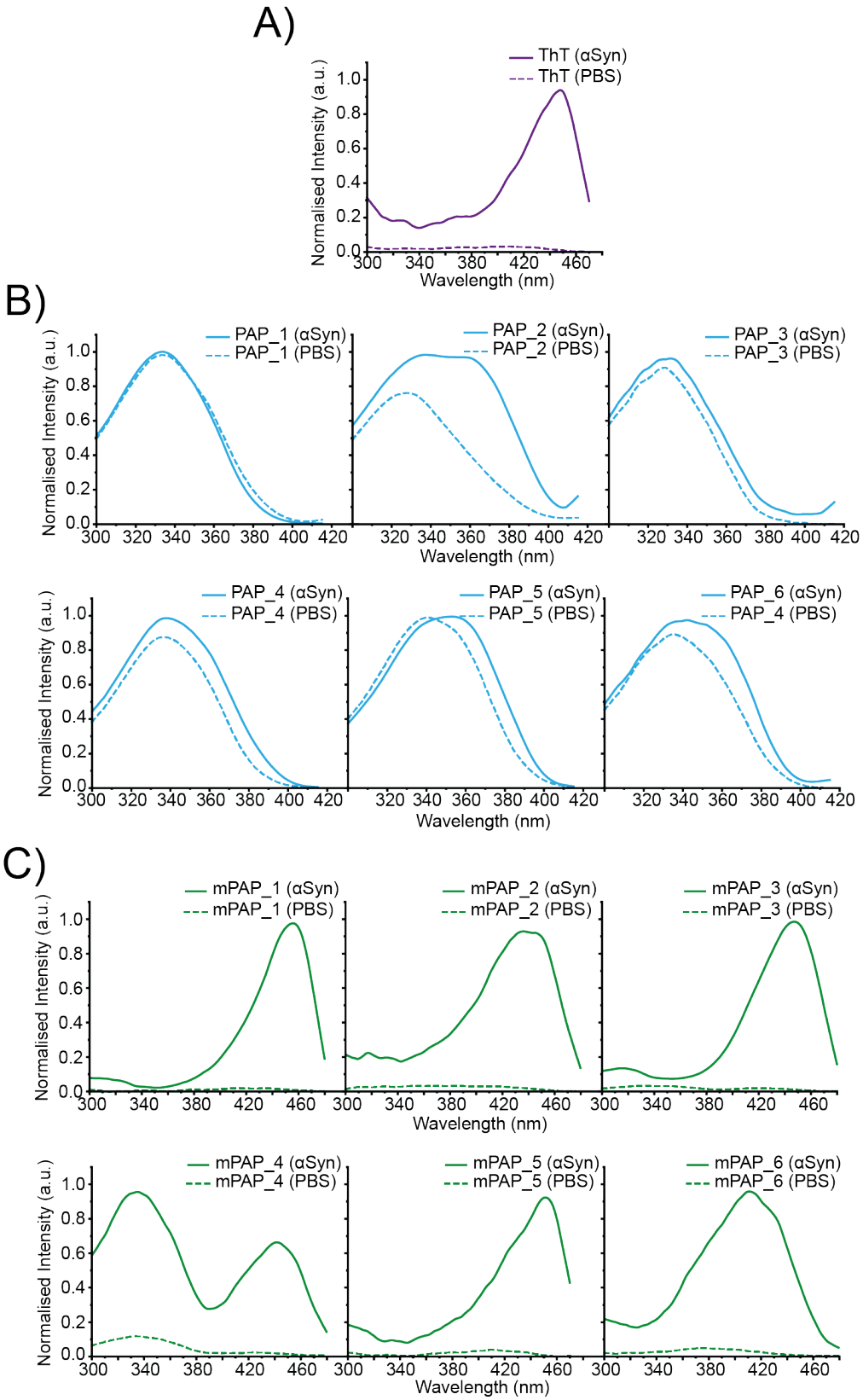

Figure S2. Bulk excitation spectra of 10 μM **A)** ThT, **B)** PAP derivatives and **C)** mPAP derivatives in PBS and with 2 μM recombinant αSyn aggregates (>96 hours). The spectra have been independently normalised relative to the maximum intensity of the dye in the presence of αSyn aggregates.

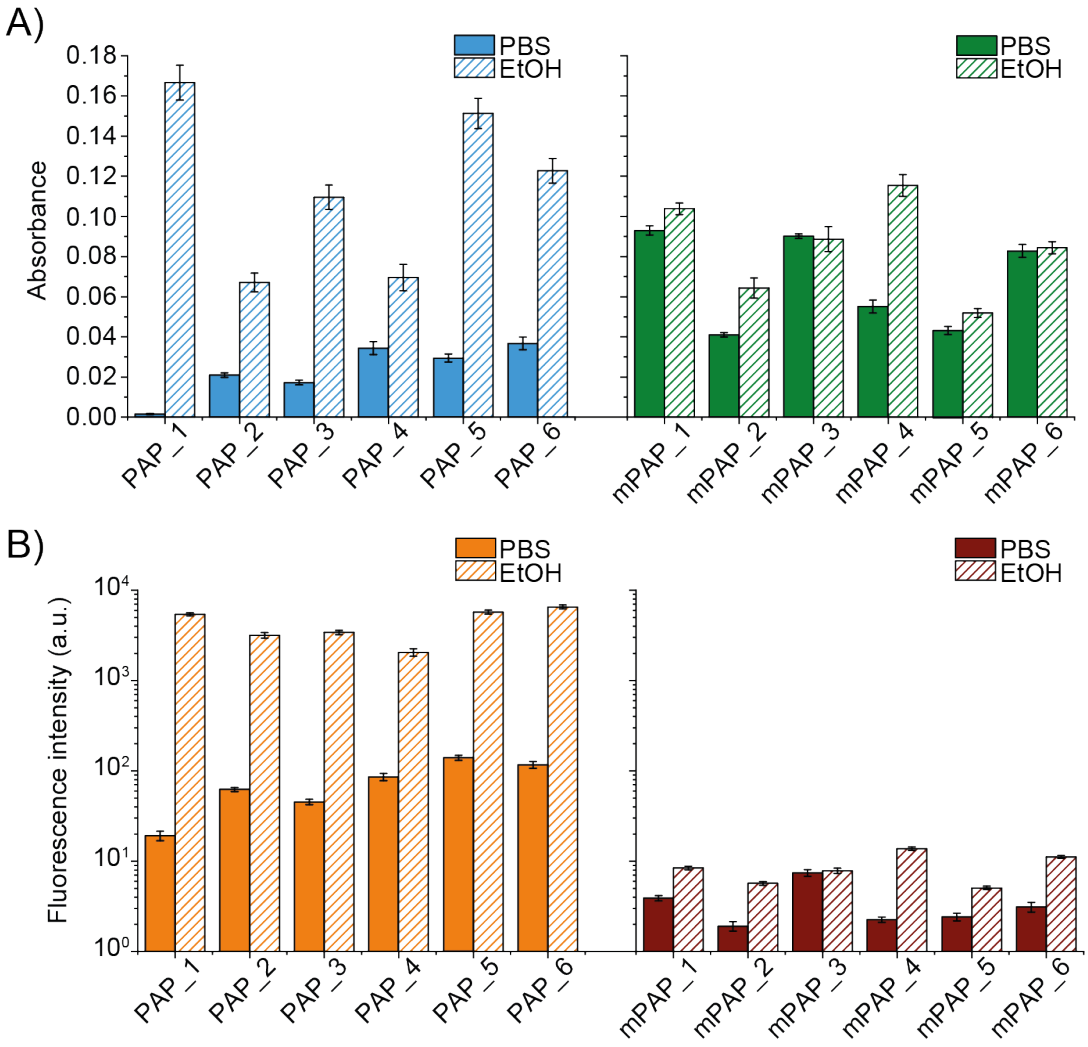

Figure S3. Bar graphs showing **A)** maximum absorbance and **B)** maximum emission intensity of 10 µM PAP and mPAP dyes in PBS and ethanol (EtOH). Error bars represent the standard deviation of n=3 separate dye preparations.

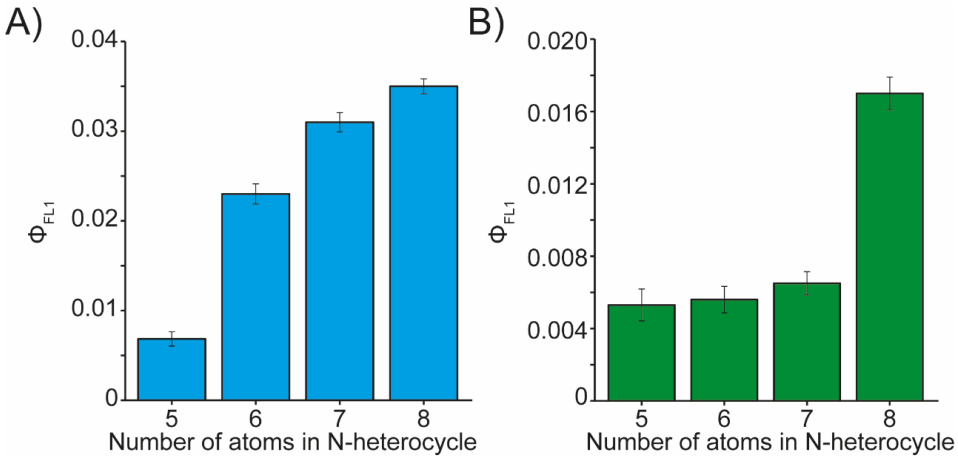

Figure S4. Bar graphs showing the relationship between Φ_{FI1} and ring size of N-heterocycle substituted **A)** PAP derivatives and **B)** mPAP derivatives. Φ_{FI1} increases with ring size in both cases. Error bars represent the standard deviation from n=3 separate dye preparations.

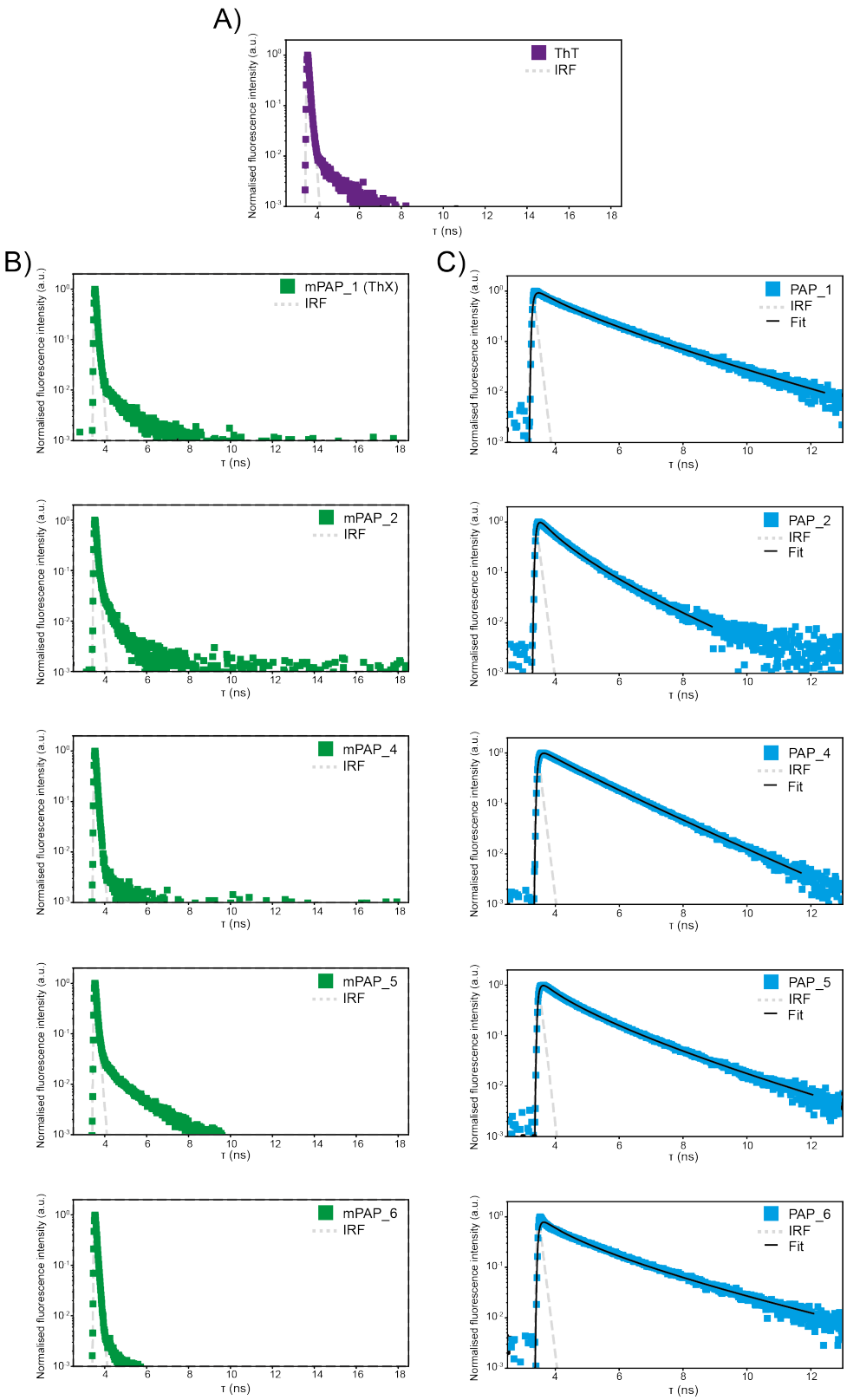

Figure S5. Fluorescence decay curves of **A)** ThT, **B)** mPAP derivatives and **C)** PAP derivatives in PBS. The grey dashed line represents the instrument response function (IRF). The fluorescence decay of the PAP derivatives were fit to a stretched exponential decay function (Supplementary Experimental Methods). This was not applied to the mPAP derivatives and ThT as the decay rate was faster than the IRF.

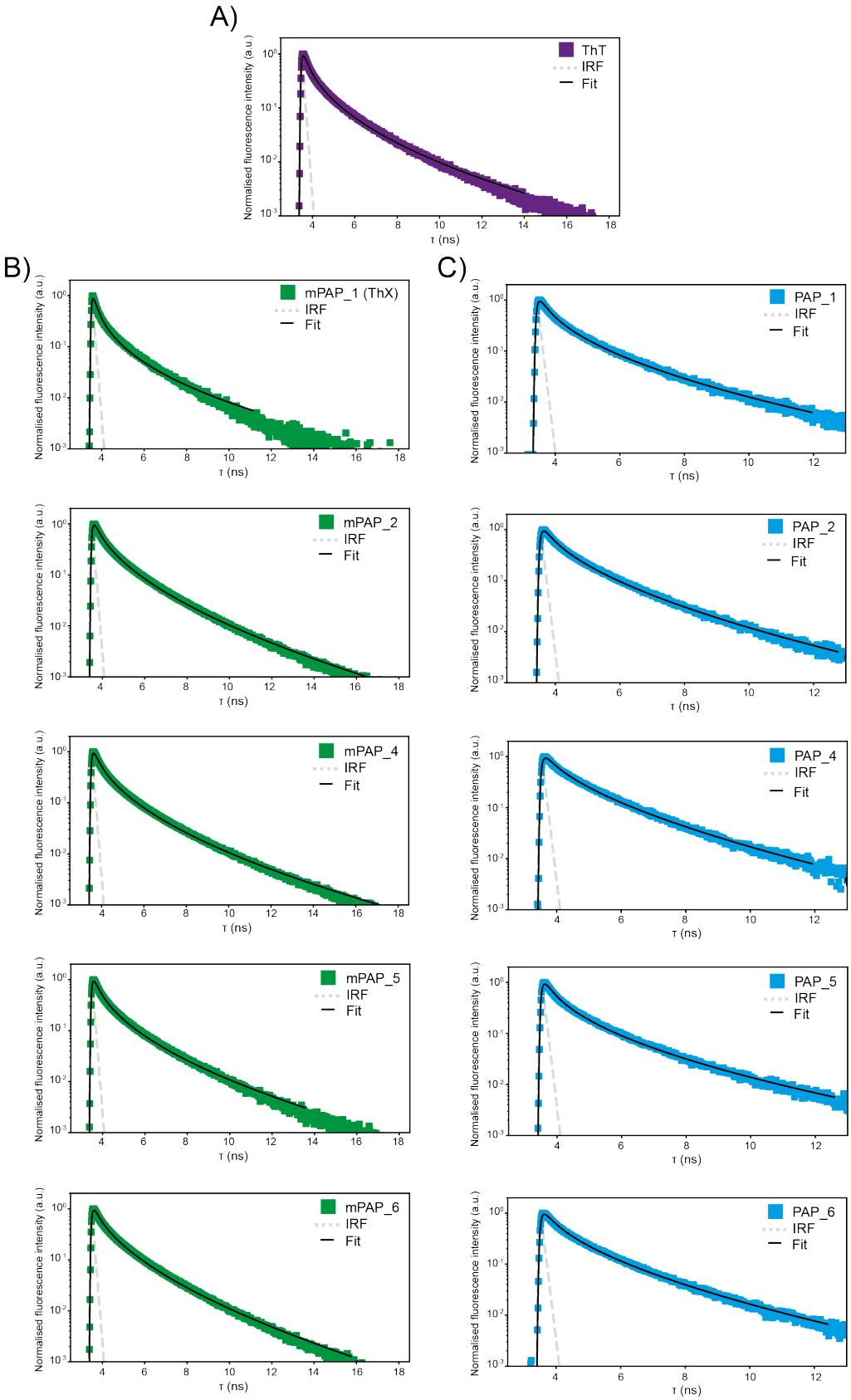

Figure S6. Fluorescence decay curves of **A)** ThT, **B)** mPAP derivatives and **C)** PAP derivatives bound to αSyn aggregates. The grey dashed line represents the instrument response function (IRF). The fluorescence decay of all dyes were fit to a stretched exponential decay function (Supplementary Experimental Methods).

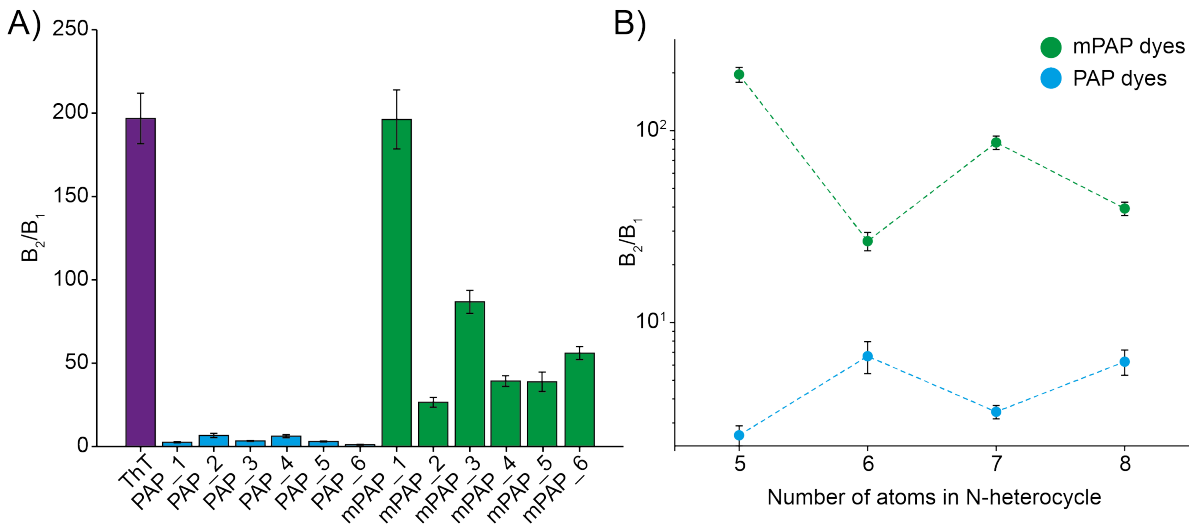

Figure S7. A) Bar graph showing the turn-on ratio, $\left(\frac{B_2}{B_1}\right)$, of ThT, PAP and mPAP derivatives **B)** Evaluation of turn-on ratio as a function of ring size of N-heterocycle substituted derivatives. No clear relationship is observed. Error bars represent the standard deviation of repeats from n=3 αSyn aggregations.

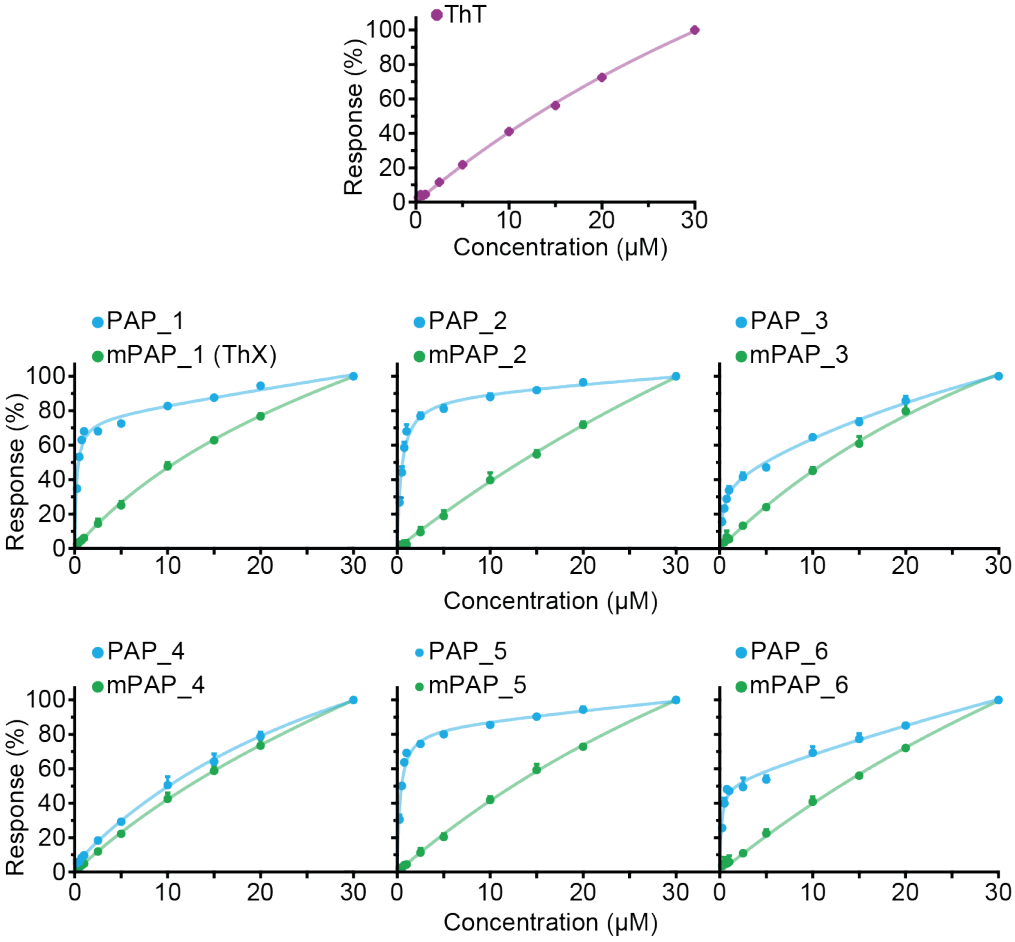

Figure S8. Binding affinity data obtained from SPR experiments of ThT, PAP and mPAP derivatives binding to surface functionalised αSyn aggregates (>96 hours). Error bars represent the standard deviation of repeats from n=3 αSyn aggregations.

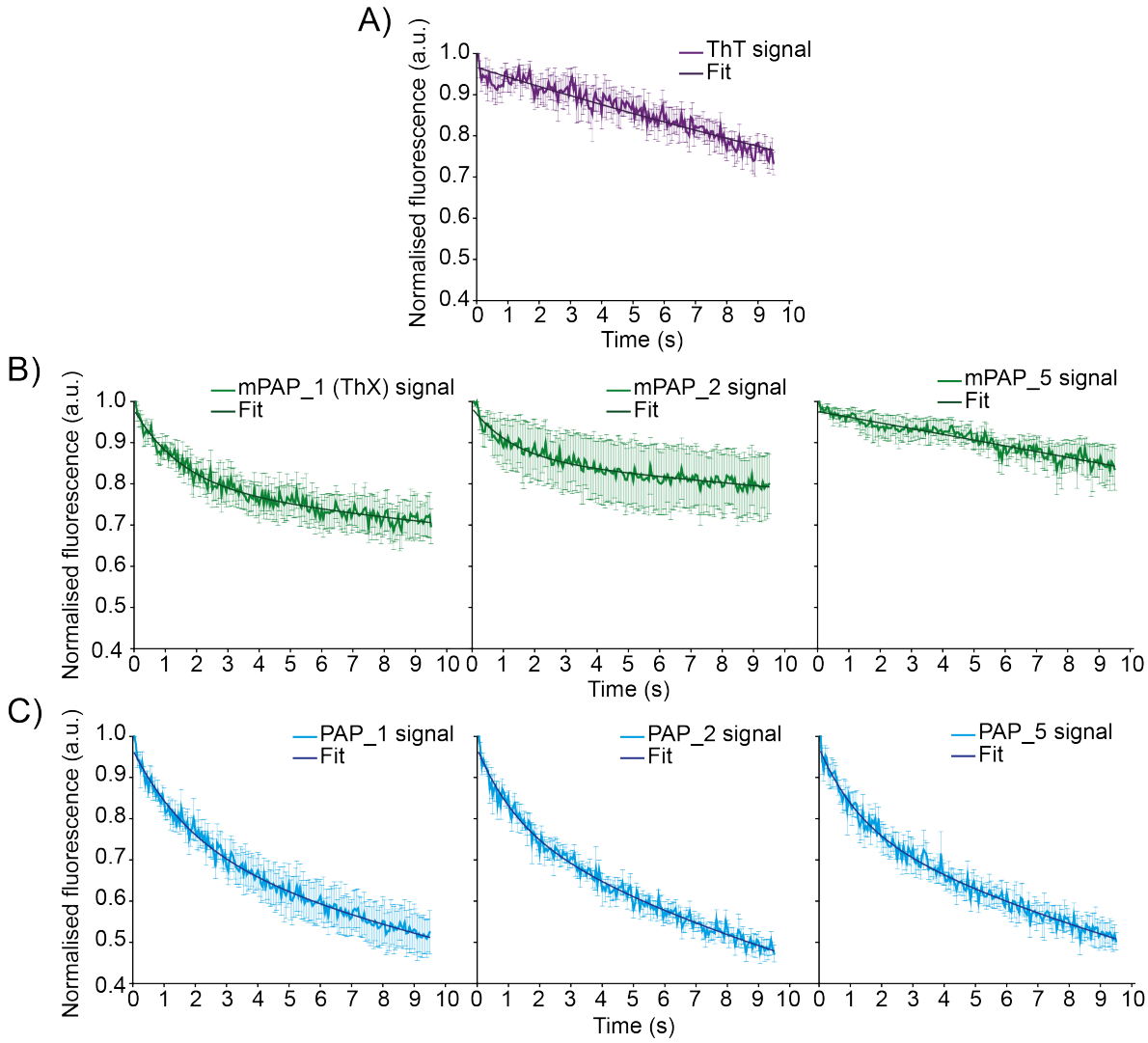

Figure S9. Mean fluorescence intensity over the total acquisition time of **A)** ThT, **B)** mPAP dyes (mPAP_1, mPAP_2, mPAP_5) and **C)** PAP dyes (PAP_1, PAP_2, PAP_5) bound to single αSyn aggregates. The error bars represent the standard deviation of intensity from ≥ 300 aggregates across n=3 separate cover-slides

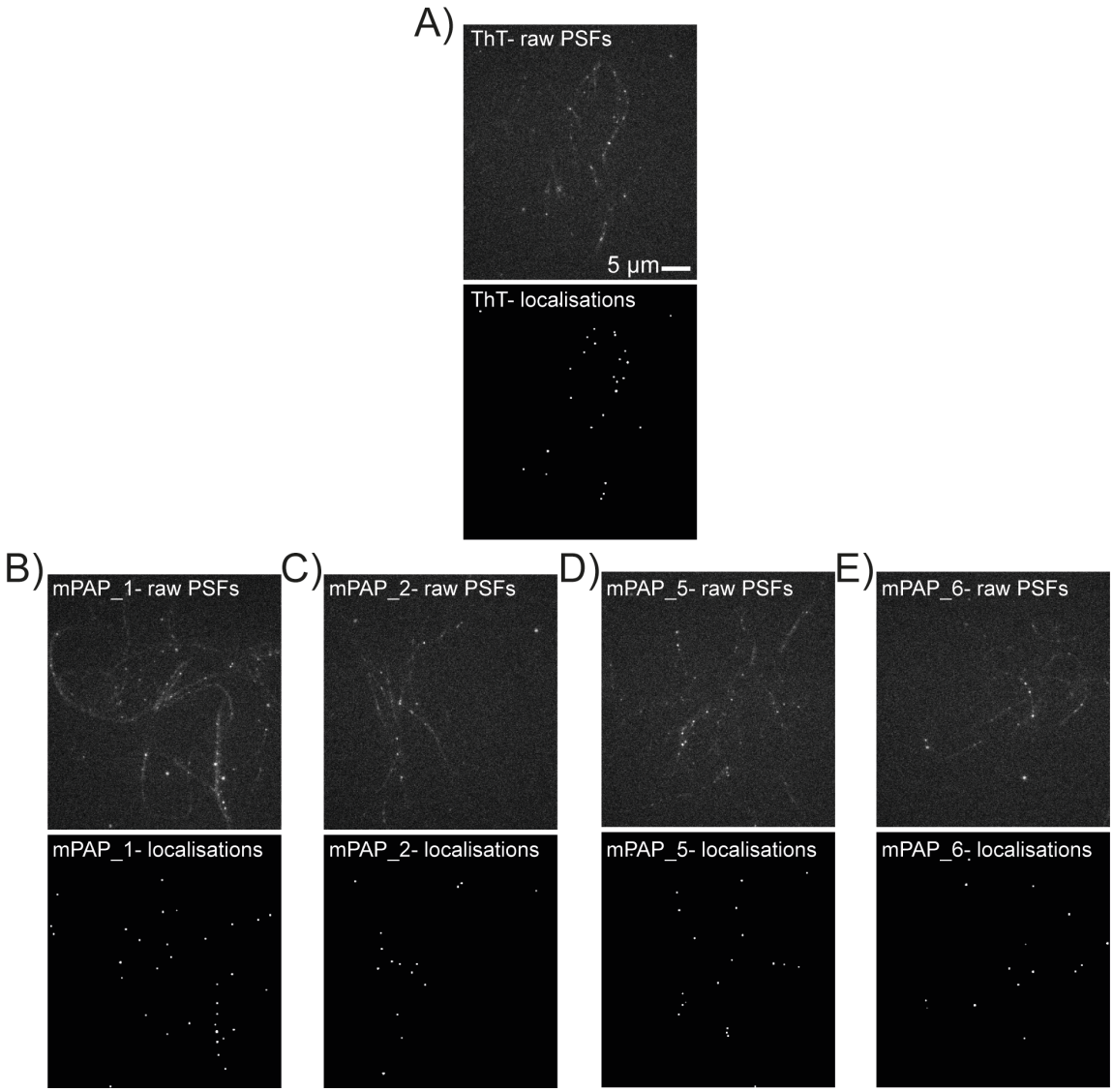

Figure S10. Single-frame images showing raw, spatially isolated molecules (top) and gaussian blurred localisations of **A)** ThT, **B)** mPAP_1 (ThX), **C)** mPAP_2, **D)** mPAP_5 and **E)** mPAP_6 undergoing TAB onto αSyn aggregates. All images are the same scale.

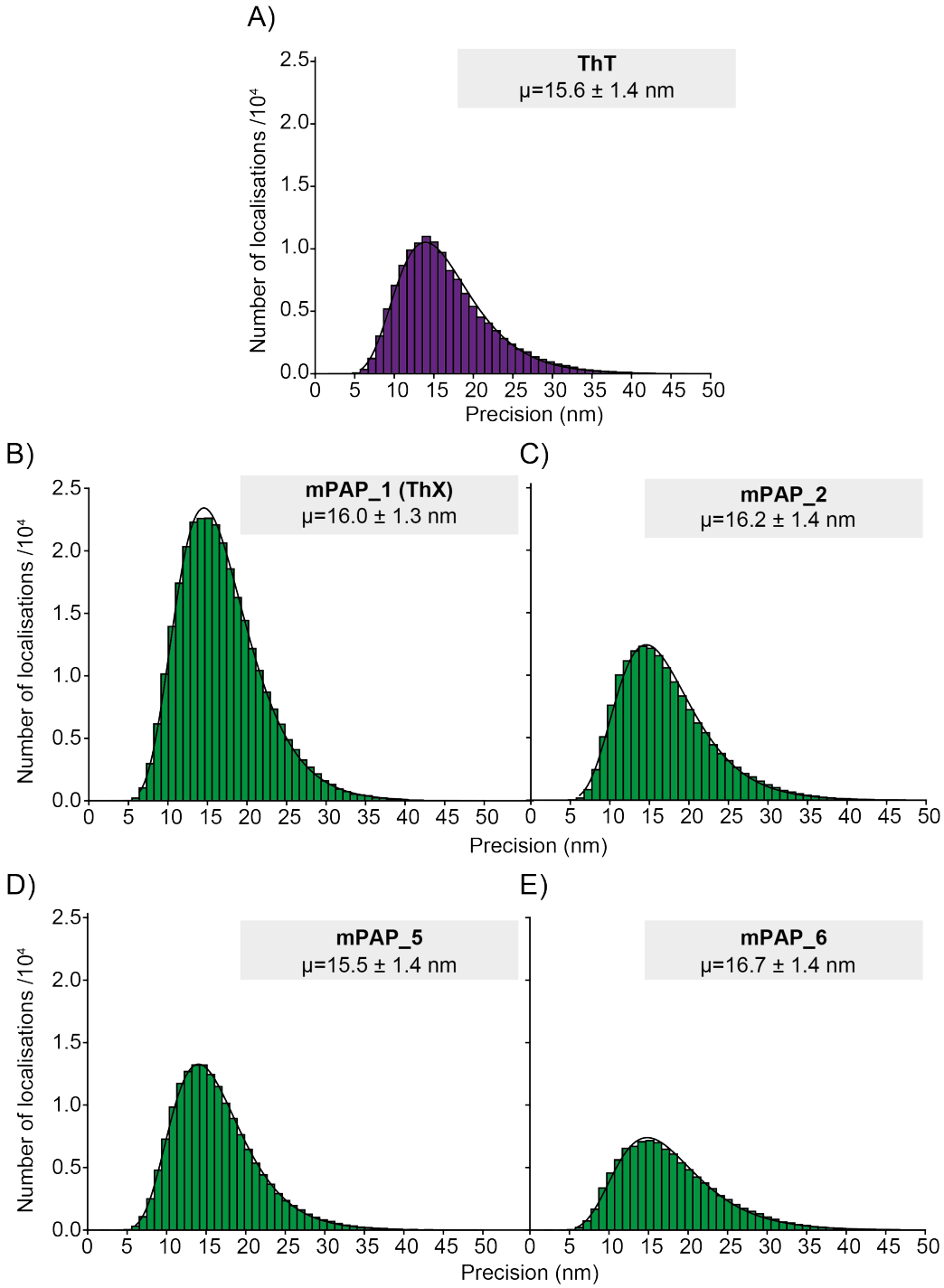

Figure S11. Histograms of the localisation precision of single emitters of **A)** ThT, **B)** mPAP_1 (ThX), **C)** mPAP_2, **D)** mPAP_5 and **E)** mPAP_6. Localisations of fiducial markers were removed prior to this analysis.

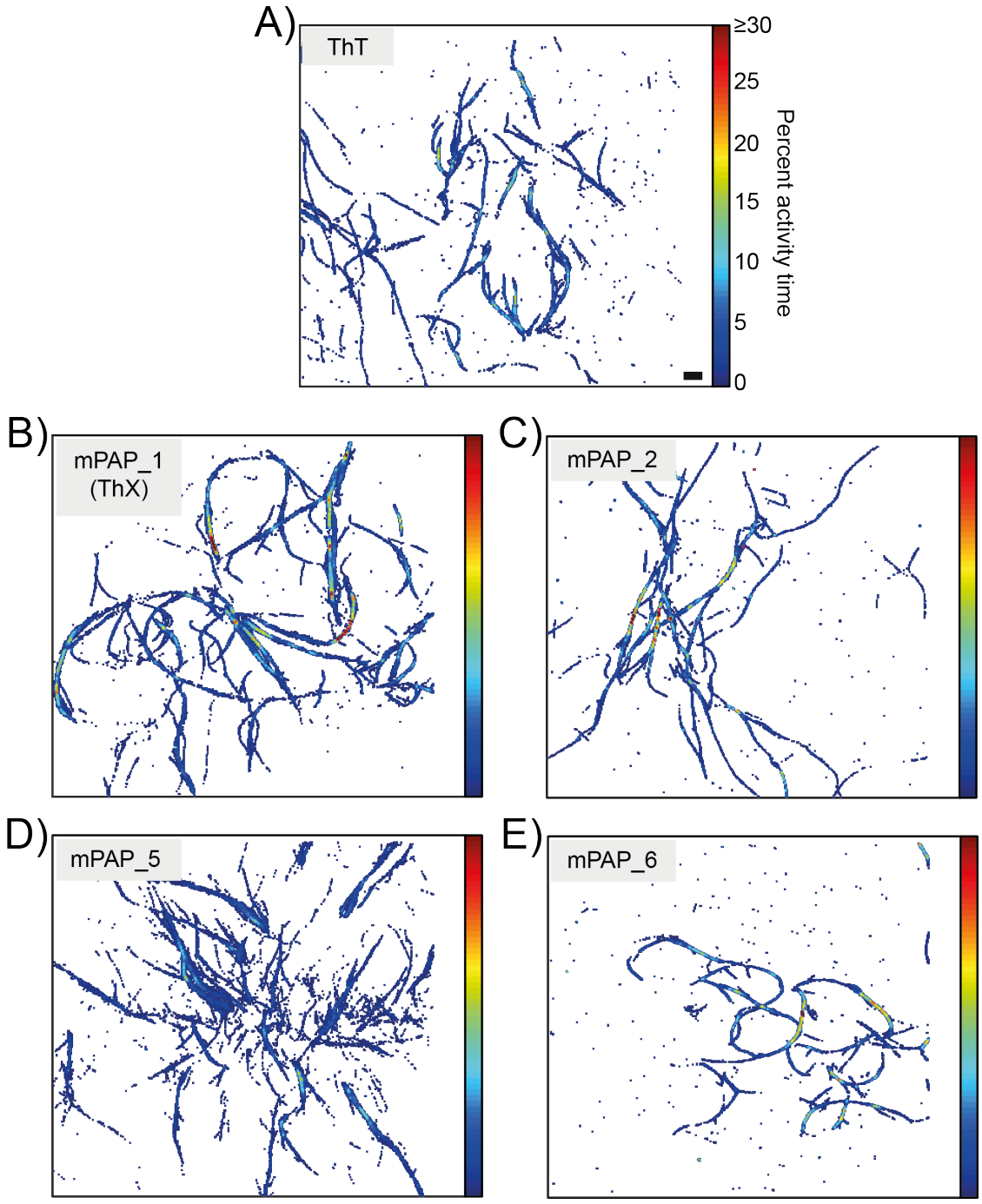

Figure S12. Representation of the percentage time super-localised pixels are active during the acquisition time of the TAB super-resolution imaging experiment of **A)** ThT, **B)** mPAP_1 (ThX), **C)** mPAP_2, **D)** mPAP_5 and **E)** mPAP_6 binding to surface adsorbed αSyn aggregates. Z intensity scale represents the binding site activity time (as indicated in A) and is the same for all figure panels. Localisations of fiducial markers were removed prior to this analysis. Scale bar =2 μm.

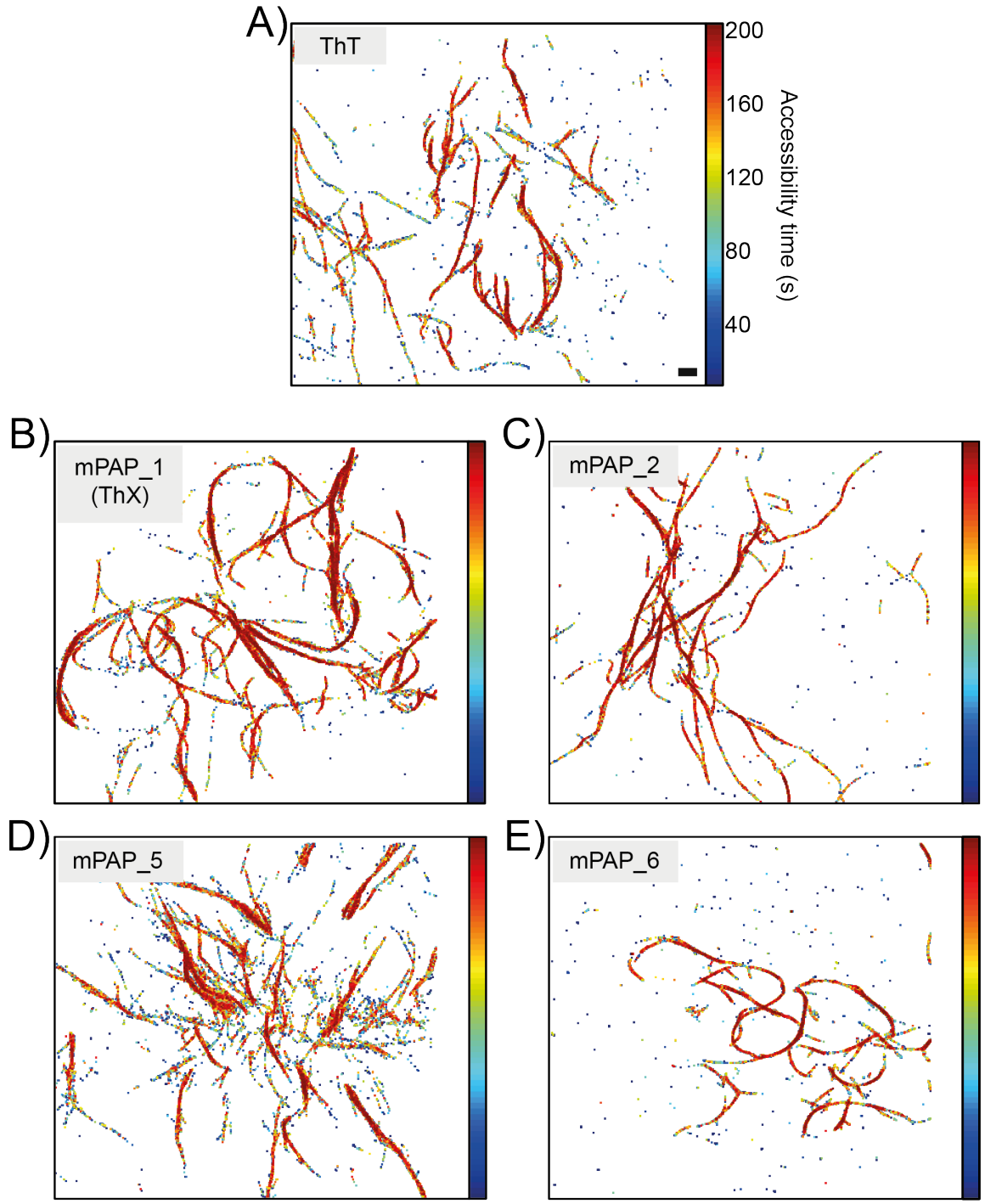

Figure S13. Representation of the total time that super-localised pixels are accessible during the acquisition time of the TAB super-resolution imaging experiment of **A)** ThT, **B)** mPAP_1 (ThX), **C)** mPAP_2, **D)** mPAP_5 and **E)** mPAP_6 binding to surface adsorbed αSyn aggregates. Z intensity scale represents the binding site activity time (as indicated in A) and is the same for all figure panels. Localisations of fiducial markers were removed prior to this analysis. Scale bar =2 μm.

Movie S1. 500-frame, raw movies of ThT, mPAP_1 (ThX), mPAP_2, mPAP_5, and mPAP_6 undergoing TAB onto surface immobilised αSyn fibrils. The frame rate is in real-time (50 fps) and scale-bar=5 μm

2. Experimental Methods

Synthesis.

General Considerations

Unless otherwise noted, all reactions have been carried out with distilled and degassed solvents under an atmosphere of dry N_2 in flame or oven-dried glassware with standard vacuum-line techniques. Toluene was purified under a positive pressure of dry argon by passage through columns of activated alumina and Q5 (Grubbs apparatus). DMSO used was reagent grade with no further purification. Chlorobenzene was distilled from CaH_2 prior to use. All workup and purification procedures were carried out with reagent grade solvents (purchased from Sigma-Aldrich) in air. Standard column chromatography techniques using ZEOprep 60/40-63 μm silica gel were used for purification. Liquids and solutions were transferred via syringe or cannula.

^1H and ^{13}C NMR spectra were recorded at room temperature on Varian Inova-instrumentation: Varian I400 (^1H NMR at 400MHz and ^{13}C NMR at 100 MHz), Varian VXR400 (^1H NMR at 400 MHz and ^{13}C NMR at 100 MHz), Varian I500 (^1H NMR at 500 MHz and ^{13}C NMR at 126 MHz) and Varian I600 (^1H NMR at 600 MHz and ^{13}C NMR at 151 MHz) using deuterium lock. Data for ^1H NMR spectra are quoted relative to chloroform as an internal standard (7.26 ppm) and data for ^{13}C NMR spectra are quoted relative to chloroform as an internal standard (77.16 ppm) and are reported in terms of chemical shift (δ ppm). Data are reported as follows: chemical shift, multiplicity (s = singlet, d = doublet, t = triplet, q = quartet, br = broad, m = multiplet), coupling constants (Hz) and integration. Infrared spectra (IR) were obtained on the Bruker TENSOR II FTIR Spectrometer and recorded in wavenumbers (cm^{-1}). Spectra can be found in the Appendix.

Melting points were obtained on a Thomas Hoover capillary melting point apparatus without correction. High Resolution Mass (HRMS) analysis was obtained using Electron Impact Ionization (EI), Chemical Ionization (CI), Electrospray (ESI) and Atmospheric Pressure Chemical Ionization (APCI) and reported as m/z (relative intensity) for the $[M]^+$, $[M+H]^+$ or $[M+Na]^+$ molecular ion.

2-amino-5-methoxybenzenethiol

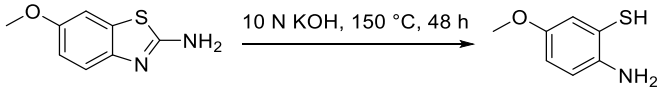

The following method was adapted from a literature procedure.[1]

To a stirring suspension of 2-amino-6-methoxybenzothiazole (12.0 g, 66.6 mmol) in water (60 mL), was added KOH (60.0 g, 1.07 mol) at room temperature. The mixture was then heated to 150 °C using a heating mantle. TLC analysis showed complete conversion after 48 h. After cooling to 0 °C, the solution was cautiously adjusted to pH 5 using concentrated HCl (36.5%). The aqueous mixture was then extracted with $CHCl_3$ (2 x 600 mL), dried using Na_2SO_4 and concentrated under reduced pressure to yield a yellow solid (9.78g, 95%). All spectral data matched those previously reported.

^{1}H NMR (400 MHz, $CDCl_3$) δ 6.66 (d, 1H, *J* = 2.6 Hz), 6.57 (d, 1H, *J* = 8.5 Hz), 6.43 (dd, 1H, *J* = 8.5, 2.6 Hz), δ 3.78 (s, 3H).

2-(4-bromophenyl)-6-methoxybenzo[*d*]thiazole

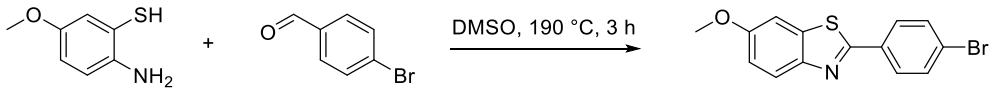

To a mixture of 2-amino-5-methoxybenzenethiol (9.78 g, 63.0 mmol) and 4-bromobenzaldehyde (11.60 g, 62.7 mmol) was added DMSO (65 mL) under an ambient atmosphere. The mixture was heated to 190 °C (pre-heated oil bath) for 3 hours. Upon cooling to room temperature, the reaction was diluted with water (400 mL) and extracted with CH_2Cl_2 (800 mL). The organics were then washed with water (2 x 400 mL), dried using Na_2SO_4, and concentrated under reduced pressure. The resulting brownish solid was then triturated using Et_2O (~ 300 mL), filtered, and washed with Et_2O (~ 100 mL). The resulting very light green solid (14.52 g, 72%) was sufficiently pure for subsequent steps.

Purification *via* chromatography was also possible when it was difficult to remove the colour using trituration. This was done by absorption onto Celite, and elution through silica using CH_2Cl_2/EtOAc/Petroleum Ether [1:1:20].

Melting point: 152-153 °C

IR (film): 2964, 1604, 1556, 1507, 1477, 1395, 1286, 1263, 1224, 1102, 1059, 1024, 967, 826 cm^{-1}.

^{1}H NMR (500 MHz, $CDCl_3$) δ 7.94 (d, *J* = 9.0 Hz, 1H), 7.91 (d, *J* = 8.5 Hz, 2H), 7.61 (d, *J* = 8.5 Hz, 2H), 7.35 (d, *J* = 2.5 Hz, 1H), 7.10 (dd, *J* = 9.0, 2.5 Hz, 1H), 3.90 (s, 3H).

^{13}C NMR (126 MHz, $CDCl_3$) δ 164.1, 158.0 148.7, 136.5, 132.7, 132.2, 128.6, 124.9, 123.8, 116.0, 104.2, 77.3, 77.0, 76.8, 55.8.

HRMS (ESI): m/z calcd for $[M+H]^+$ $C_{14}H_{11}BrN_2OS$: 319.9745 matched on $[M+H]^+$ at 319.9759

General Procedure A - Buchwald–Hartwig Amination

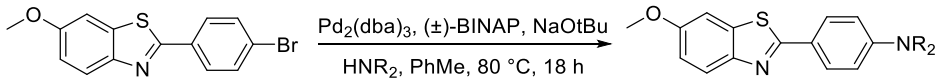

An oven-dried microwave vial was charged with 2-(4-bromophenyl)-6-methoxybenzo[*d*]thiazole (160 mg, 0.5 mmol), $Pd_2(dba)_3$ (4.6 mg, 1 mol%), BINAP (9.2 mg, 3 mol%), and NaOtBu (67.2mg, 0.7 mmol). The vial was then evacuated and purged with N_2 (x3) and capped immediately. The amine (0.6 mmol) and toluene (3 mL) were added and the mixture was heated to 80 °C for 18 hours. The mixture was cooled to room temperature, diluted with ethyl acetate (5 mL), and filtered through Celite. The filtrate was concentrated, and the residue was triturated with diethyl ether (20 mL). The solid was filtered and rinsed with cold Et_2O (2 x 10 mL) to give the desired product. In all cases the triturated products were sufficiently pure for analysis.

Scale-up of this procedure was equally as efficient using either a sealed tube or a round bottomed flask equipped with a condenser.

6-methoxy-2-(4-(pyrrolidin-1-yl)phenyl)benzo[*d*]thiazole (PAP_1)

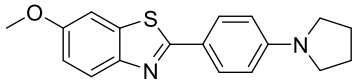

Prepared according to General Procedure A (60% yield)

Melting point: 215-216 °C

IR (film): 2968, 2845, 1606, 1553, 1463, 1427, 1318, 1264, 1183, 1029, 1005, 970, 861 cm^{-1}.

^1H NMR (400 MHz, $CDCl_3$) δ = 7.89 (d, *J* = 8.8 Hz, 2H), 7.85 (d, *J* = 8.9 Hz, 1H), 7.31 (d, *J* = 2.6 Hz, 1H), 7.03 (dd, *J* = 8.9, 2.6 Hz, 1H), 6.59 (d, *J* = 8.8 Hz, 2H), 3.88 (s, 3H), 3.37 (m, 4H), 2.05 (m, 4H).

^{13}C NMR (125 MHz, $CDCl_3$): δ = 160.2, 150.5, 142.9, 142.4, 129.2, 122.1, 116.1, 114.4, 108.2, 49.3, 41.0, 19.0.

HRMS (ESI): m/z calcd for $[M+H]^+$ $C_{18}H_{18}N_2OS$: 311.1218 matched on $[M+H]^+$ at 311.1217

6-methoxy-2-(4-(piperidin-1-yl)phenyl)benzo[*d*]thiazole (PAP_2)

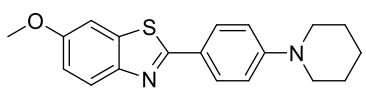

Prepared according to General Procedure A (60% yield)

Melting point: 167-168 °C

IR (film): 2934, 1606, 1464, 1284, 1224, 1127, 1061, 1026, 967, 916, 820 cm^{-1}.

^1H NMR (500 MHz, $CDCl_3$) δ = 7.90 (d, *J* = 8.9 Hz, 2H), 7.87 (d, *J* = 9.0 Hz, 1H), 7.32 (d, *J* = 2.6 Hz, 1H), 7.04 (dd, *J* = 8.9, 2.6 Hz, 1H), 6.94 (d, *J* = 8.9 Hz, 2H), 3.88 (s, 3H), 3.31 (t, *J* =5.5 Hz, 5H), 1.70 (m, 4H), 1.63 (m, 2H).

^{13}C NMR (125 MHz, $CDCl_3$): δ = 166.1, 157.2, 153.3, 148.9, 136.0, 128.5 123.5, 123.0, 115.0, 104.4, 55.8, 49.3, 25.5, 24.4.

HRMS (ESI): m/z calcd for $[M+H]^+$ $C_{19}H_{21}N_2OS$: 325.1375 matched on $[M+H]^+$ at 325.1370.

2-(4-(azepan-1-yl)phenyl)-6-methoxybenzo[*d*]thiazole (PAP_3)

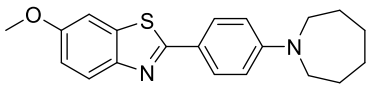

Prepared according to General Procedure A (70% yield)

Melting point: 180-182 °C

IR (film): 2933, 2848, 1606, 1558, 1487, 1463, 1285, 1262, 1193, 1028, 1008, 962, 892 cm^{-1}.

^1H NMR (500 MHz, $CDCl_3$): δ = 7.86 (m, 3H), 7.31 (d, *J* = 2.6 Hz, 1H), 7.03 (m, 1H), 6.71 (d, *J* = 8.9 Hz, 2H), 3.87 (s, 3H), 3.52 (m, 4H), 1.82 (m, 4H), 1.56 (m, 4H).

^{13}C NMR (400 MHz, $CDCl_3$): δ = 166.6, 157.0, 150.7, 149.0, 135.8, 128.8, 122.7, 120.8, 114.8, 111.0, 104.4, 55.8, 49.4, 27.5, 27.0.

HRMS (ESI): m/z calcd for $[M+H]^+$ $C_{20}H_{23}N_2OS$: 339.1531 matched on $[M+H]^+$ at 339.1523

2-(4-(azocan-1-yl)phenyl)-6-methoxybenzo[*d*]thiazole (PAP_4)

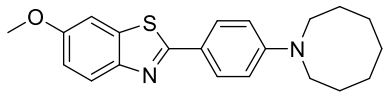

Prepared according to General Procedure A (65% yield)

Melting point: 175-177 °C

IR (film): 2924, 2851, 1606, 1559, 1463, 1399, 1223 1189, 1061, 1027, 961, 892 cm^{-1}.

^1H NMR (500 MHz, $CDCl_3$): δ = 7.88 (d, *J* = 7.5 Hz, 2H), 7.85 (d, *J* = 9 Hz, 1H), 7.31 (s, 1H), 7.03 (d, *J* = 9 Hz, 1H), 6.71 (d, *J* = 7.5 Hz, 2H), 3.88 (s, 3H), 3.53 (m, 4H), 1.79 (m, 4H), 1.68 (m, 2H), 1.60 (m, 4H).

^{13}C NMR (126 MHz, $CDCl_3$): δ = 166.6, 157.3, 149.9, 149.3, 135.8, 128.7, 122.6, 120.7, 114.8, 111.1, 104.4, 55.8, 51.0, 27.1, 27.0, 26.7.

LRMS (ESI): m/z calcd for $[M+H]^+$ $C_{21}H_{24}N_2OS$: 353.1688 matched on $[M+H]^+$ at 353.1699

4-(6-methoxybenzo[*d*]thiazol-2-yl)-*N*,*N*-dimethylaniline (PAP_5)

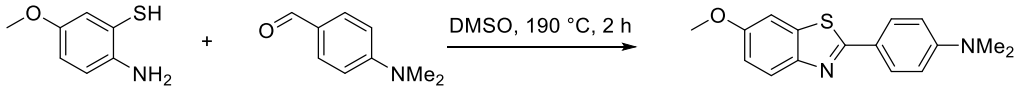

To a mixture of 4-(dimethylamino)benzaldehyde (1.49 g, 10 mmol) and 2-amino-5-methoxybenzenethiol (1.55 g, 10 mmol) was added DMSO (20 mL) under a ambient atmosphere. The reaction was then stirred at 190 °C for 2 hours. The reaction mixture was the cooled to room temperature, water (15 mL) added and the solid formed was collected *via* filtration. The solid cake was dissolved in DCM (15 mL), dried over Na_2SO_4, filtered and the concentrated under reduced pressure. The resulting light pink solid (1.85 g, 65%) was sufficiently pure for further use.

Melting point: 176-178 °C

IR (film): 2936, 1610, 1559, 1532, 1434, 1369, 1263, 1225, 1064, 1025, 965, 945, 850 cm^{-1}.

^1H NMR (500 MHz, CDCl3) δ 7.91 (d, *J* = 8.9 Hz, 2H), 7.86 (d, *J* = 8.9 Hz, 1H), 7.32 (d, *J* = 2.5 Hz, 1H), 7.04 (dd, *J* = 8.9, 2.6 Hz, 1H), 6.74 (d, *J* = 8.9 Hz, 2H), 3.88 (s, 3H), 3.05 (s, 6H).

^{13}C NMR (126 MHz, CDCl3) δ 159.9, 150.5, 145.4, 142.4, 129.3, 122.0, 116.2, 115.1, 108.3, 105.2, 97.8, 49.3, 33.6.

HRMS (EI): m/z calcd for $[M+H]^+$ $C_{16}H_{16}N_2OS$ 285.1062 matched on $[M+H]^+$ at 285.1049

4-(4-(6-methoxybenzo[*d*]thiazol-2-yl)phenyl)morpholine (PAP_6)

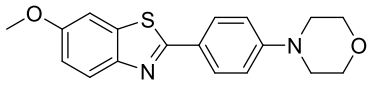

Prepared according to General Procedure A (65% yield)

Melting point: 240-241 °C

IR (film): 2953, 2838, 1606, 1560, 1524, 1489, 1441, 1382, 1287, 1226, 1024, 963, 863 cm^{-1}.

^1H NMR (500 MHz, $CDCl_3$) δ 7.94 (d, *J* = 8.3 Hz, 2H), 7.89 (d, *J* = 9.0 Hz, 1H), 7.33 (s, 1H), 7.05 (d, *J* = 8.9 Hz, 1H), 6.95 (d, *J* = 8.4 Hz, 2H), 3.87 (s, 3H), 3.87 (m, 4H), 3.27 (m, 4H).

^{13}C NMR (151 MHz, $CDCl_3$) δ 165.7, 157.4, 152.7, 148.9, 136.0, 128.5, 124.9, 123.1, 114.8, 104.3, 66.7, 55.8, 48.3.

HRMS (ESI): m/z calcd for $[M+H]^+$ $C_{18}H_{19}N_2O_2S$: 327.1167 matched on $[M+H]^+$ at 327.1171.

General Procedure B - Preparation of *N*-Methylated Ammonium Salts

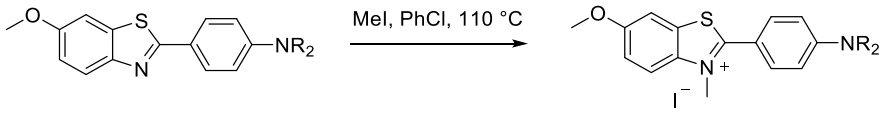

To an oven dried 1 dram vial equipped with magnetic stir bar was added the specified amine (0.2 mmol) and iodomethane (1 mL). Chlorobenzene (1.5 mL) was added and the vial sealed with a Teflon sealed screw cap. After heating to 110 °C for 18 hours, the reaction was cooled to room temperature and the residue triturated with Et_2O. The pure mono *N*-methylated product was collected by filtration.

Upon scale-up of this procedure the Teflon capped vial was replaced by an appropriately sized sealed tube.

6-methoxy-3-methyl-2-(4-(pyrrolidin-1-yl)phenyl)benzo[*d*]thiazol-3-ium iodide (mPAP_1 (ThX))

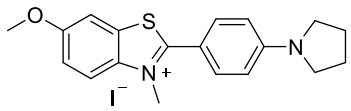

Prepared according to General Procedure B (90% yield)

Melting point: 208-210 °C

IR (film): 2972, 2864,1602, 1537, 1504,1482, 1441, 1298, 1272, 1065, 1034, 1016, 859 cm^{-1}.

^1H NMR (500 MHz, $CDCl_3$): δ = 7.94 (dd, *J* = 9.3, 1.8 Hz, 1H), 7.89 (d, *J* = 2.2 Hz, 1H), 7.35 – 7.28 (m, 1H), 6.71 – 6.64 (m, 2H), 4.43 (d, *J* = 1.8 Hz, 3H), 3.90 (d, *J* = 1.8 Hz, 3H), 3.40 (m, 3H), 2.08 (m, 4H).

^{13}C NMR (126 MHz, $CDCl_3$) δ 170.9, 159.4, 151.5, 136.7, 132.6, 129.7, 129.7, 128.6, 126.4, 118.9, 117.4, 112.6, 110.4, 106.7, 56.7, 47.9, 40.0, 25.4.

HRMS (CI): m/z calcd for $[M-I]^+$ $C_{19}H_{21}N_2OS$: 325.1369 $[M-I]^+$ at 325.1382

6-methoxy-3-methyl-2-(4-(piperidin-1-yl)phenyl)benzo[*d*]thiazol-3-ium iodide (mPAP_2)

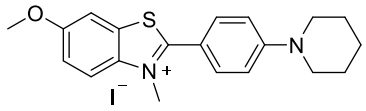

Prepared according to General Procedure B (80% yield)

Note: Double methylation was significant in this example. A reaction time of 4 hours and product purification by chromatography (direct concentration of PhCl, then 2.5-10% $MeOH/CHCl_3$) allowed for the pure title compound to be obtained.

Melting point: 188-190 °C

IR (film): 2930, 1598, 1501, 1480, 1400, 1243, 1205, 1125, 1037, 818 cm^{-1}.

^1H NMR (500 MHz, $CDCl_3$): δ = 7.98 (d, *J* = 9.2 Hz, 1H), 7.80 (d, *J* = 9.1 Hz, 2H), 7.75 (d, *J* = 2.5 Hz, 1H), 7.34 (dd, *J* = 9.2, 2.4 Hz, 1H), 7.00 (d, *J* = 9.1 Hz, 2H), 4.48 (s, 3H), 3.95 (s, 3H), 3.50 (m, 4H), 1.72 (m, 6H).

^{13}C NMR (126 MHz, $CDCl_3$) δ 170.8, 159.7, 154.3, 136.8, 132.8, 129.9, 119.2, 117.7, 113.9, 111.6, 106.5, 56.6, 48.2, 39.9, 29.8, 25.4, 24.3.

HRMS (CI): m/z calcd for $[M-I]^+$ $C_{20}H_{23}N_2OS$: 339.1526 matched on $[M-I]^+$ at 339.1517

2-(4-(azepan-1-yl)phenyl)-6-methoxy-3-methylbenzo[*d*]thiazol-3-ium iodide (mPAP_3)

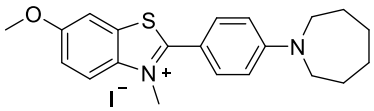

Prepared according to General Procedure B (70% yield)

Melting point: 180-182 °C

IR (film): 3006, 2928, 2854, 1598, 1538, 1503, 1438, 1303, 1270, 1196, 973, 865, 822 cm^{-1}.

^1H NMR (500 MHz, $CDCl_3$): δ = 7.95 (d, *J* = 9.3 Hz, 1H), 7.90 (s, 1H), 7.75 (d, *J* = 9.0 Hz, 2H), 7.29 – 7.24 (m, 1H), 6.84 (d, *J* = 9.0 Hz, 2H), 4.45 (s, 3H), 3.91 (s, 3H), 3.58 (t, *J* = 6.0 Hz, 4H), 1.84 (m, 4H), 1.69 (m, 2H), 1.58 (m, 2H).

^{13}C NMR (126 MHz, $CDCl_3$) δ 170.8, 159.5, 153.1, 136.8, 132.8, 129.7, 119.0, 117.5, 112.0, 110.5, 106.7, 56.7, 49.8, 40.0, 27.0, 26.7.

LRMS (CI): m/z calcd for $[M-I]^+$ $C_{21}H_{25}N_2OS$ 353.1682 matched on $[M-I]^+$ at 353.1675

2-(4-(azocan-1-yl)phenyl)-6-methoxy-3-methylbenzo[*d*]thiazol-3-ium iodide (mPAP_4)

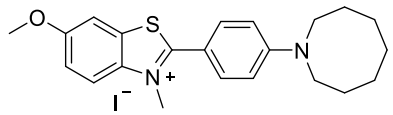

Prepared according to General Procedure B (80% yield)

Melting point: 110-112 °C

IR (film): 3006, 2926, 2690, 1598, 1538, 1481, 1401, 1304, 1271, 1036, 1018, 968, 867cm^{-1}.

^1H NMR (500 MHz, $CDCl_3$) δ 7.95 (d, *J* = 9.2, 1H), 7.77 (d, *J* = 9.2, 2H), 7.75 (s, 1H), 7.31 (d, *J* = 9.2 Hz, 1H), 6.85 (d, *J* = 9.2, 2H), 4.45 (s, 3H), 3.93 (s, 3H), 3.60 (t, *J* = 4.3 Hz, 4H), 1.83 (d, *J* = 3.2 Hz, 2H), 1.67 – 1.50 (m, 8H).

^{13}C NMR (126 MHz, $CDCl_3$): δ = 170.9, 159.5, 152.4, 136.8, 132.7, 129.7, 119.0, 117.5, 112.4, 110.4, 106.6, 77.2, 56.7, 51.6, 39.9, 26.9, 26.8, 26.4, 26.1.

HRMS (CI): m/z calcd for [M-I]+ $C_{22}H_{27}N_2OS$ 367.1839 matched on $[M-I]^+$ at 367.1837

2-(4-(dimethylamino)phenyl)-6-methoxy-3-methylbenzo[d]thiazol-3-ium iodide (mPAP_5)

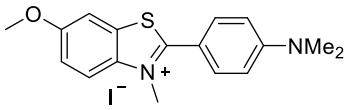

Prepared according to General Procedure B (95% yield)

Melting point: 207-209 °C

IR (film): 1601, 1506, 1482, 1386, 1272, 1232, 1208, 1065, 822 cm^{-1}.

^1H NMR (500 MHz, $CDCl_3$): δ = 7.97 (d, *J* = 9.2 Hz, 1H), 7.84 – 7.76 (m, 3H), 7.31 (dd, *J* = 9.2, 2.6 Hz, 1H), 6.83 (d, *J* = 9.1 Hz, 2H), 4.47 (s, 3H), 3.93 (s, 3H), 3.14 (s, 6H).

^{13}C NMR (126 MHz, $CDCl_3$): δ 171.0, 159.6, 153.9, 136.8, 132.6, 129.9, 119.1, 117.7, 112.3, 111.0, 106.6, 56.6, 40.2, 40.0.

HRMS (CI): m/z calcd for [M-I]+ $C_{17}H_{19}N_2OS$: 299.1213 matched on $[M-I]^+$ at 299.1216

6-methoxy-3-methyl-2-(4-morpholinophenyl)benzo[*d*]thiazol-3-ium iodide (mPAP_6)

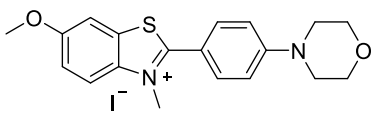

Prepared according to General Procedure B (75% yield)

Melting point: 237-239 °C

IR (film): 2851, 1599, 1502, 1481, 1438, 1400, 1302, 1273, 1242, 1113, 1035, 927, 825 cm^{-1}.

^1H NMR (500 MHz, $CDCl_3$) δ = 7.96 (d, *J* = 9.0 Hz, 1H), 7.89 (d, *J* = 2.5 Hz, 1H), 7.86 (d, *J* = 8.6 Hz, 2H), 7.31 (dd, *J* = 9.0, 2.5 Hz, 1H), 7.04 (d, *J* = 8.6 Hz, 2H), 4.46 (s, 3H), 3.91 (s, 3H), 3.87 (t, *J* = 4.9 Hz, 4H), 3.41 (t, *J* = 4.9 Hz, 4H).

^{13}C NMR (126 MHz, $CDCl_3$) δ 159.8, 154.5, 136.7, 132.7, 130.6, 119.6, 117.8, 114.2, 113.5, 110.0, 106.7, 66.4, 56.7, 46.9, 39.8.

HRMS (CI): m/z calcd for $[M-I]^+$ $C_{19}H_{21}IN_2O_2S$: 341.1318 matched on $[M-I]^+$ at 341.1326

Preparation of αSyn aggregates. The purification of monomeric wild-type αSyn from Escherichia coli was performed following a published protocol.[2] αSyn aggregates used for bulk photophysical characterization and binding affinity measurements were generated as previously described[3]. Briefly, monomeric αSyn was diluted into 50 mM sodium phosphate (pH 7.4) to reach a final concentration between 150 and 300 μM. Samples were incubated at 45°C for in total 72 hours whilst stirring at maximum speed with a Teflon flea. The aggregation reaction was sonicated at 24-hour intervals (3 cycles of 10 seconds at 30% power (Branson digital Sonifer, model 250, Branson, St Louis MO, USA). Finally, the

aggregation mixture was aliquoted, flash frozen in liquid N_2 and stored at -80 °C. The αSyn concentration stated in the different experiments is reported as the monomer equivalent concentration.

For all single-aggregate and super-resolution imaging experiments, αSyn aggregates were generated by diluting monomeric αSyn into filtered (0.2 μm syringe filter, Whatman, 6780-1302) PBS buffer containing 0.01% NaN_3 to a final concentration of 70 μM. The solution was then incubated in the dark at 37 °C with constant shaking (200 rpm) for the time stated in the experiment.

Preparation of dye stock solutions. Stock solutions of PAP derivatives, mPAP derivatives and ThT (AnaSpec, AS-88306) were prepared by dissolving the solid into dimethyl sulfoxide (DMSO, Sigma Aldrich, 276855) to a concentration of 10 mM, these were stored in the dark at -80 °C. The stock solutions were diluted into filtered (0.02 μm syringe filter, Whatman, 6809-1102) PBS (pH 7.4) to the required concentration for experiments. The diluted dye solutions were then sonicated (5 minutes) and filtered (0.02 μm syringe filter, Whatman, 6809-1102). The diluted solutions were stored in the dark at 4 °C for a maximum of a week after preparation.

Photophysical characterization. Samples were placed into a quartz fluorescence cuvette (Hellma Analytics, 3×3 mm) and bulk fluorescence spectra were recorded using a fluorescence spectrophotometer (Cary Eclipse, Varian) in which emission was collected perpendicular to direction of propagating excitation. Initial fluorescence spectra of the PAP derivatives, mPAP derivatives and ThT at multiple concentrations (0.25-25 μM) were recorded free in PBS (pH 7.4) and in the presence of late stage αSyn aggregates (~2 μM, >96 hours). Replicates were made with n=3 separately prepared dye samples. UV-Vis absorption spectra were collected by placing samples in a quartz transmission cuvette (Hellma Analytics, 1 cm path length) and measured with an absorption spectrometer (Cary 400, Varian). Buffer blanks were collected for both fluorescence and absorption spectra and used for background correction. Several photophysical quantities of the PAP derivatives, mPAP derivatives and ThT were determined from ensemble absorption and emission data using a custom Matlab script. These included absorption maxima (λ_{abs}), emission maxima (λ_{em}), molar extinction coefficient (ε), fluorescence quantum yield (Φ_{Fl}) and brightness (B). ε was determined from a calibration curve of the UV-vis absorbance and sample path length using the Beer–Lambert law with solutions of known concentrations. Φ_{Fl} of the dyes were determined by referencing against either quinine sulfate in sulfuric acid (Φ_{Fl}= 0.5) for the

PAP derivatives or rhodamine 101 (Sigma-Aldrich, 83694) in ethanol (Φ_{Fl}= 1.0) for the mPAP derivatives and ThT and discrepancies in absorbance and solvent refractive index were corrected for.[4]

Surface plasmon resonance. SPR studies were performed at 25°C using a Biacore T200 in HBS-EP+ buffer (10 mM HEPES, 150 mM sodium chloride, 3mM EDTA, and 0.05% v/v surfactant P20 in MQ water; filtered through a vacuum driven 0.22 µm filter system from Millipore) containing 5% v/v DMSO. αSyn aggregates, prepared as described prior, were covalently coupled to a Research Grade CM5 sensor chip (BIAcore) via primary amino functionalities of the fibrils using the amine coupling kit provided by BIAcore. For surface coating, αSyn was injected at a concentration of 2.8 µM in 10 mM sodium acetate buffer (pH 4.0) at a flow rate of 10 µL/min for 12 minutes. A second flow cell was treated identically including all immobilisation chemistry but without αSyn to function as reference for analysis. 30 µM dye solutions were prepared by dilution 10 mM dye stock solutions into HBS-EP+ buffer to 30 µM. The concentration series (30-0.1 µM) was then prepared by further diluting the 30 µM solution. To correct for the DMSO content in the samples, a solvent correction assay was performed at the beginning and at the end of each measurement set. After stabilisation of the baseline, response units for each dye sample were acquired by using a flow rate of 30 µL/min for 60 seconds. Dissociation time was set to 400 seconds. No further regeneration step was needed. The measurements of each dye concentration series were conducted in a randomised order and the 10 µM sample was measured a second time after the whole concentration series of the dye to prove consistency. In between the measurements of different dyes, a 5 µM ThT sample was measured as control. The whole SPR measurement set for each dye was repeated at least three times on different flow cells with fresh immobilised αSyn aggregates and newly prepared concentration series. All data were solvent corrected, and reference subtracted. Equilibrium binding analysis was performed by normalising the obtained binding levels at the equilibrium from each concentration series and averaging the normalised values over the replicates ($n \geq 3$). The averaged values were then plotted as a function of concentration to obtain K_D.

Slide preparation for fluorescence imaging and fluorescence lifetime characterisation. Glass cover-slides (VWR, 631-1570) for single-aggregate fluorescence imaging were cleaned for 1 hour using an argon plasma (PDC-002, Harrick Plasma). Frame-Seal slide chambers (9 x 9 mm, Bio-Rad, Hercules, CA, product number SLF-0201) were attached to the cover-slide and the surface incubated with poly-l-lysine (50 µL, PLK, Sigma-Aldrich,

0.1% w/v, P820) for 30 minutes. The slide was then washed three times with filtered (0.2 μm syringe filter, Whatman, 6780-1302) PBS prior to imaging.

Fluorescence lifetime characterisation. Fluorescence lifetime measurements were performed on a MicroTime200 confocal microscope (PicoQuant) with time-correlated single photon counting (TCSPC) capability operated by SymphoTime software. A ps-pulsed 407 nm diode laser at 40 MHz repetition rate was used for excitation and focused through an objective lens (60×, UPlanSApo, NA 1.2, water-immersion, Olympus). Fluorescence light was collected through the same objective and focussed through a pin-hole (30 μm) then collimated and detected by a single-photon avalanche photodiode through a suitable spectral filter (425 nm LP/485 nm LP, Chroma). The integration time was varied to obtain sufficient signal. TCSPC data was histogrammed with 16 ps bin width. The IRF was measured experimentally under the same conditions using a fluorescein solution saturated with KI in dilute KOH as sample and the full width at half maximum was found to be approximately 130 ps.

Analysis of the obtained decay curves was performed via iterative re-convolution approach with stretched exponential as decay law (Equation 1) using a custom-built python script.
A stretched exponential function was used as model decay law to account for the observed decay complexity.

$$I(t)=\int_0^t IRF(t')\cdot I_0 \exp\left[-\left(\frac{t-t'}{\tau}\right)^{\beta}\right]dt' \qquad (1)$$

Where I(t) is fluorescence intensity at time t, t' is the dummy variable of integration, τ is the lifetime constant and β is the stretching parameter.

Microscope set-up for single-aggregate imaging. Imaging was performed on a bespoke total internal reflection fluorescence microscope using a 405 nm excitation laser (LBX-405-50-CIR-PP, Oxxius), which was passed through a quarter wave plate (WPQ05M-405, Thorlabs) aligned parallel to the optical axis at the edge of an objective lens (60x Plan Apo TIRF, NA 1.45 oil-immersion, Nikon Corporation), mounted on an inverted optical microscope (Eclipse TE2000-U, Nikon Corporation). Fluorescence emission was also collected by the same objective and selected by the presence of a dichroic (ZT 405/532 rpc) and subsequently passed through an emission filter (FF01-480/40/25) and focused by a tube lens onto an EMCCD camera (Evolve 512, Photometrics). Micromanager software was used to control the microscope[5].

Microscope set-up for super-resolution imaging. Imaging was performed on a bespoke total internal reflection fluorescence microscope using a 488 nm excitation laser (iBeam-SMART, Toptica). The beam was circularly polarized using quarter-wave plates specific to each wavelength and then expanded, collimated and aligned parallel to the optical axis at the edge of an objective lens (100× Plan Apo TIRF, NA 1.49 oil-immersion, Nikon Corporation) mounted on an inverted optical microscope (Ti-E, Eclipse, Nikon Corporation). Fluorescence emission was collected by the same objective lens and separated from excitation light using a dichroic mirror (Di01-R405/488/561/635, Semrock) and passed through appropriate emission filters (LP02-568RS-25, FF01-587/35-25, Semrock). The fluorescence was then expanded (1.5 ×) and focussed onto an electron-multiplying charge-coupled device (EMCCD, Evolve 512 Delta, Photometrics) with an electron multiplication gain of 250 ADU/photon operating in frame transfer mode. The effective pixel size was 107 nm. The instrument was automated using the open-source software micro-manager (v. 1.4) and the data displayed using the ImageJ software (v. 1.52d). Movies of single mPAP emitters undergoing TAB on αSyn aggregates were collected for 10,000 frames at a rate of 50 fps (20 ms exposure).

Single-aggregate fluorescence imaging. αSyn fibrils (72-hour, 70 μM) were diluted into filtered (0.2 μm syringe filter, Whatman, 6780-1302) PBS in low-binding tubes (Eppendorf AG, Hamburg, Germany) to a final concentration of 1 μM prior to imaging. Pre-diluted solutions of ThT, PAP or mPAP derivatives (500 μM) were further diluted to the desired imaging concentration (500 pM-250 μM for concentration dependence, 5 μM for all other imaging experiments). The diluted fibrils (50 μL) were incubated on clean, PLK coated glass cover-slides for 10 minutes. The solution was then pipetted up and down vigorously to maximise adherence of the protein to the surface following which the slide was washed three times with filtered PBS. A solution of ThT, PAP derivative or mPAP derivative (50 μL) was then added and the slide imaged immediately. 200-frame image stacks were recorded on the microscope set-up described above in frame-transfer mode at 20 frames per second with an exposure time of 50 ms. Each pixel was equal to 241 nm. Three cover-slides and 27 separate fields of view per slide were collected for each condition. To correct for any fluorescent artefacts caused by the cover-slides or any of the solutions being used, dye solutions (5 μM, 50 μL) in PBS without αSyn were imaged for each experiment and used as blanks.

Analysis of single-aggregate images. The mean intensity of each pixel across 200-frame image stacks were calculated to form a single-frame average intensity projection. An intensity threshold was applied (Equation 2) to segment single-aggregates.

$$\text{Threshold} = \frac{(I_{mean} + I_{SD})}{2} \quad (2)$$

I_{mean} is the mean pixel intensity and I_{SD} is the standard deviation pixel intensity of the image. The mean pixel intensity per segmented aggregate in ADU/photon was then calculated and converted to detected photons by dividing by the total camera gain (35.7 ADU/photon).

Super-resolution imaging. αSyn fibrils (72-hour, 70 μM) were diluted into filtered (0.2 μm syringe filter, Whatman, 6780-1302) PBS in low-binding tubes (Eppendorf AG, Hamburg, Germany) to a final concentration of 2 μM prior to imaging. Pre-diluted solutions of ThT or mPAP derivative (500 μM) were further diluted to the desired imaging concentration (1 μM). Gold nanoparticles in PBS (100 nm, 753688, Sigma-Aldrich) were used as fiducial markers and were diluted to 2 μM and incubated on clean, PLK coated glass cover-slides for 5 minutes. The slide was then washed three times with filtered PBS. The diluted fibrils (50 μL) were then incubated on the cover-slide for 10 minutes. Following this, the solution was then pipetted up and down vigorously to maximise adherence of the protein to the surface following which the slide was washed three times with filtered PBS. A solution of mPAP derivative or ThT (50 μL) in PBS was then added and the slide imaged immediately. 10,000-frame image stacks were recorded on the microscope set-up described above in frame-transfer mode at 50 frames per second with an exposure time of 20 ms. To correct for any fluorescent artefacts caused by the cover-slides or any of the solutions being used, dye solutions (1 μM, 50 μL) in PBS without αSyn were imaged for each experiment and used as blanks. Super-resolution images were reconstructed using the Drift Calculator and PeakFit package (GDSC SMLM, University of Sussex) in ImageJ, using a difference of Gaussian filter, signal strength=40, minimum photon count=150, precision=50. Localisations in the images in Figure 4 are represented as width=precision.

Analysis of TAB data. Several parameters were extracted from the localisation data using a custom Matlab script. The percentage activity ($\%_{active}$) per super-localised pixel was determined by Equation 2:

$$\%_{active} = \left(\frac{N}{t_{tot}}\right) \times 100 \quad (3)$$

in which *N* is the number of fluorophores and t_{tot} is the acquisition time. The number of fluorophores was determined by temporally-grouping localisations under the condition that 20 ms dark-time between localisations determined separation of fluorophores.

The binding site accessibility time (t_{access}) was calculated by Equation 4:

$$t_{access}=1+(t_{end}-t_{start}) \quad (4)$$

t_{start} and t_{end} are the time of first and last localisations respectively.

3. Appendix

2-(4-bromophenyl)-6-methoxybenzo[*d*]thiazole

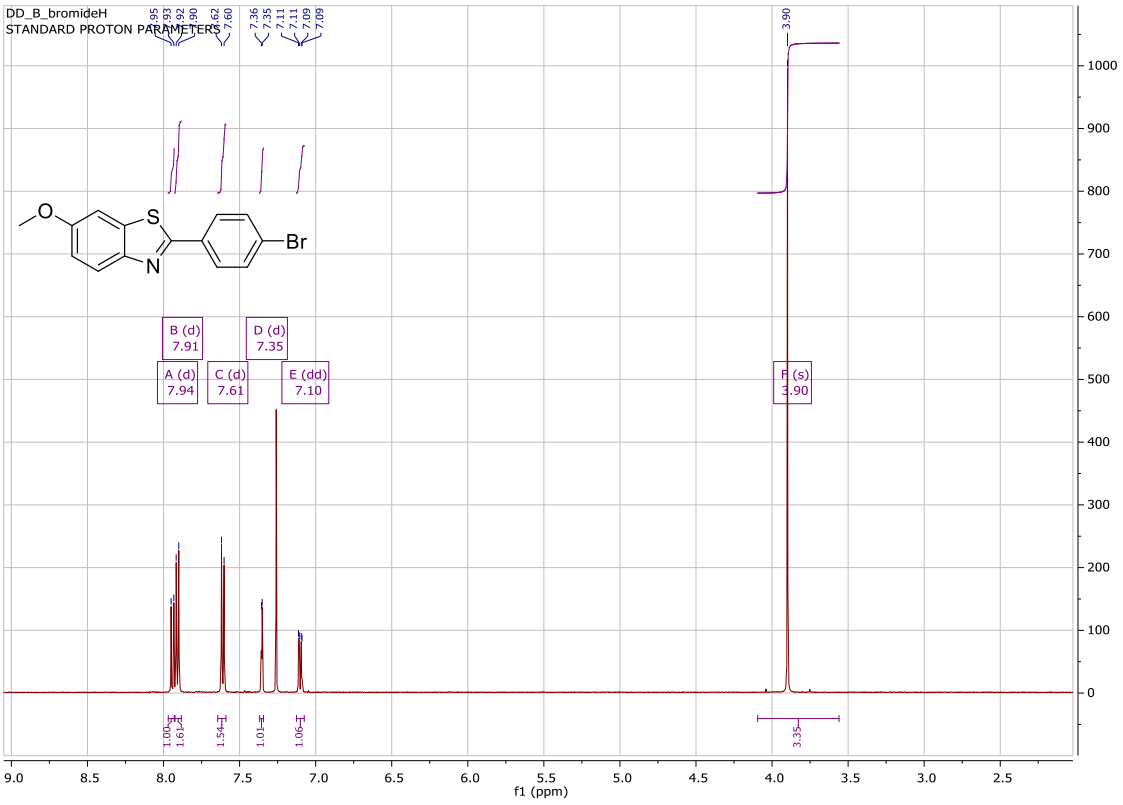

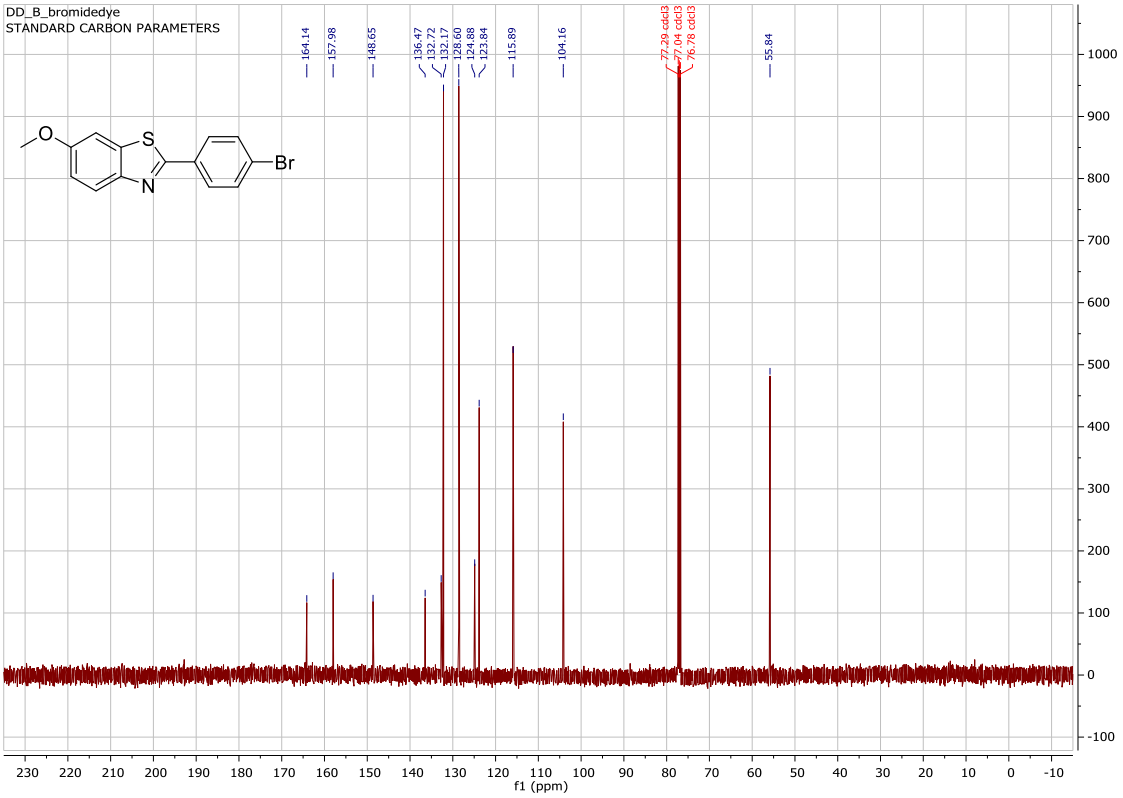

6-methoxy-2-(4-(pyrrolidin-1-yl)phenyl)benzo[*d*]thiazole (PAP_1)

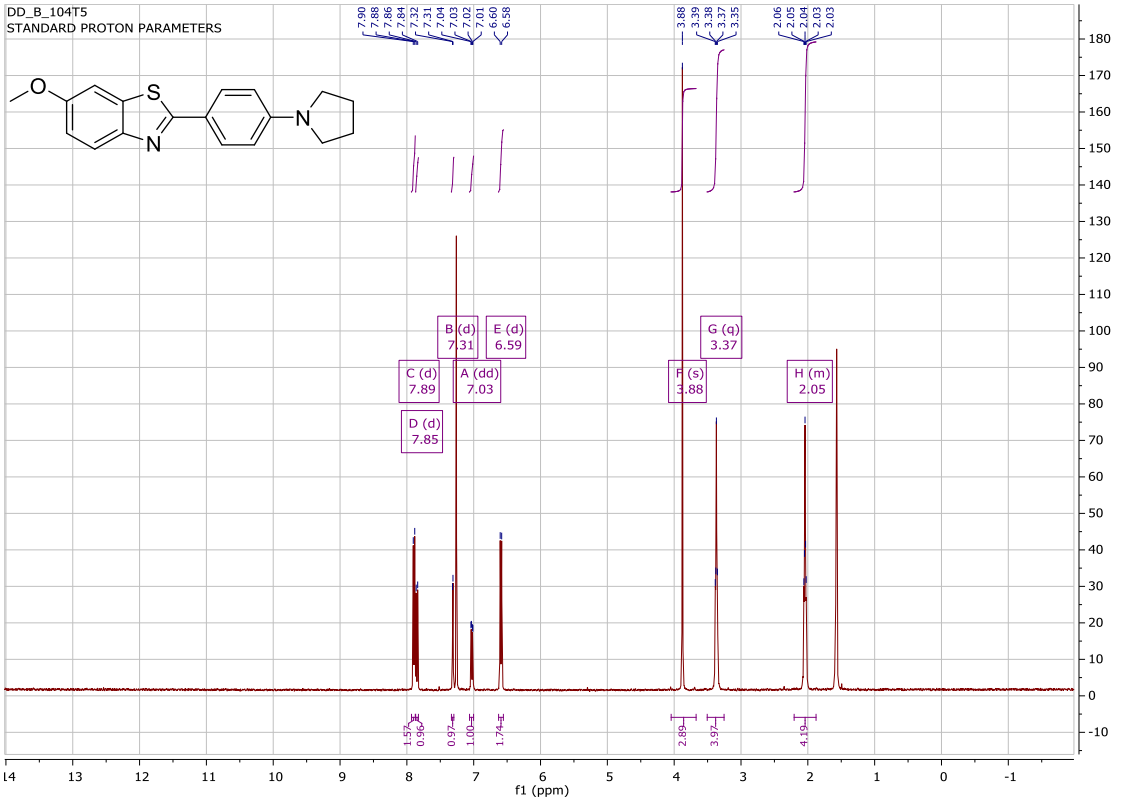

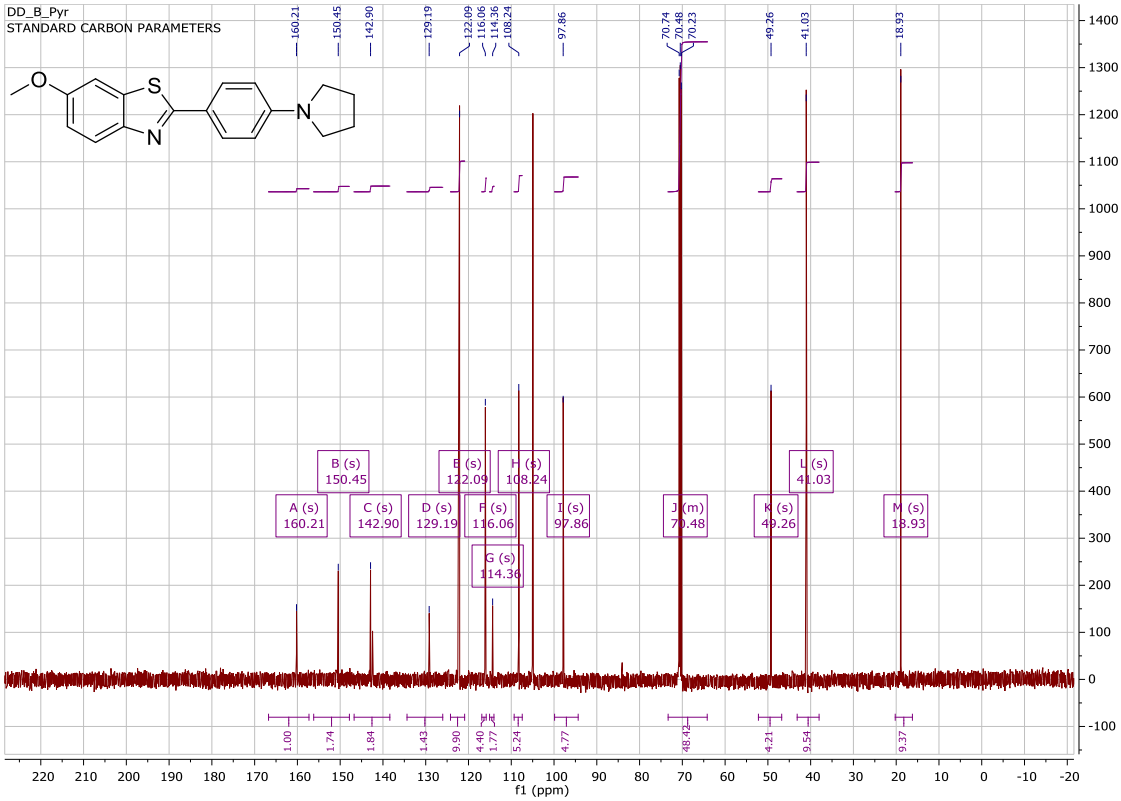

6-methoxy-2-(4-(piperidin-1-yl)phenyl)benzo[*d*]thiazole (PAP_2)

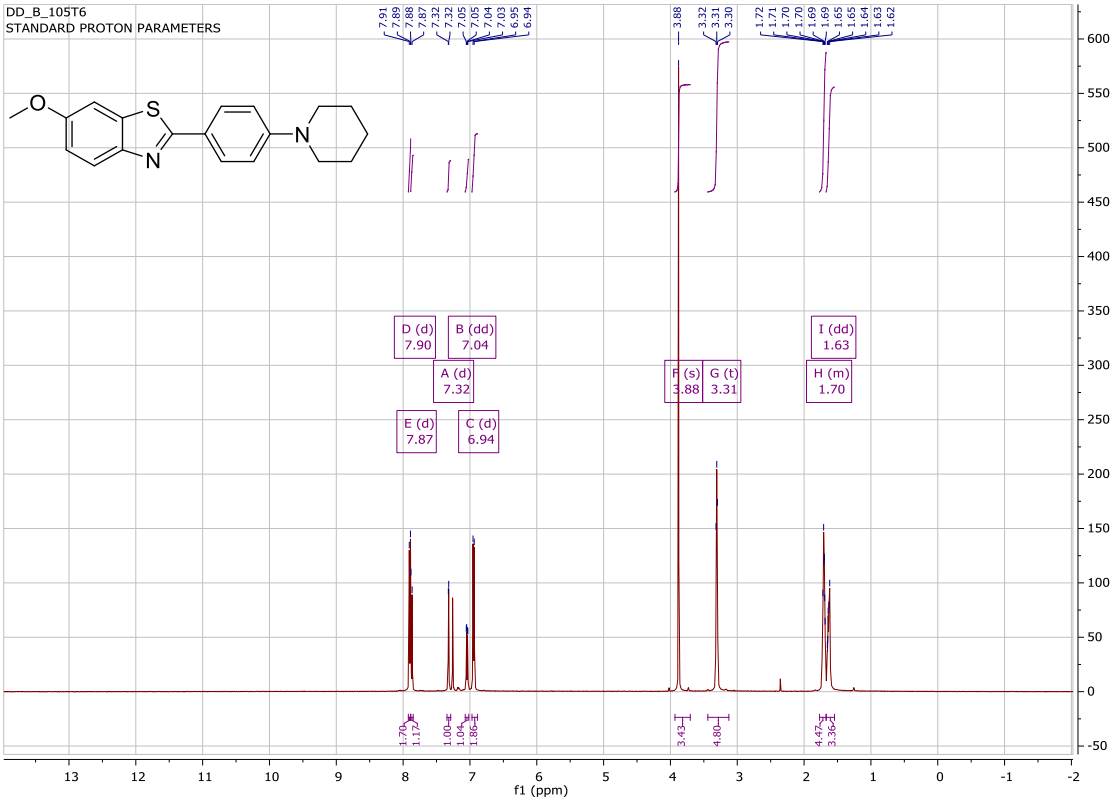

2-(4-(azepan-1-yl)phenyl)-6-methoxy-3-methylbenzo[*d*]thiazol-3-ium iodide (PAP_3)

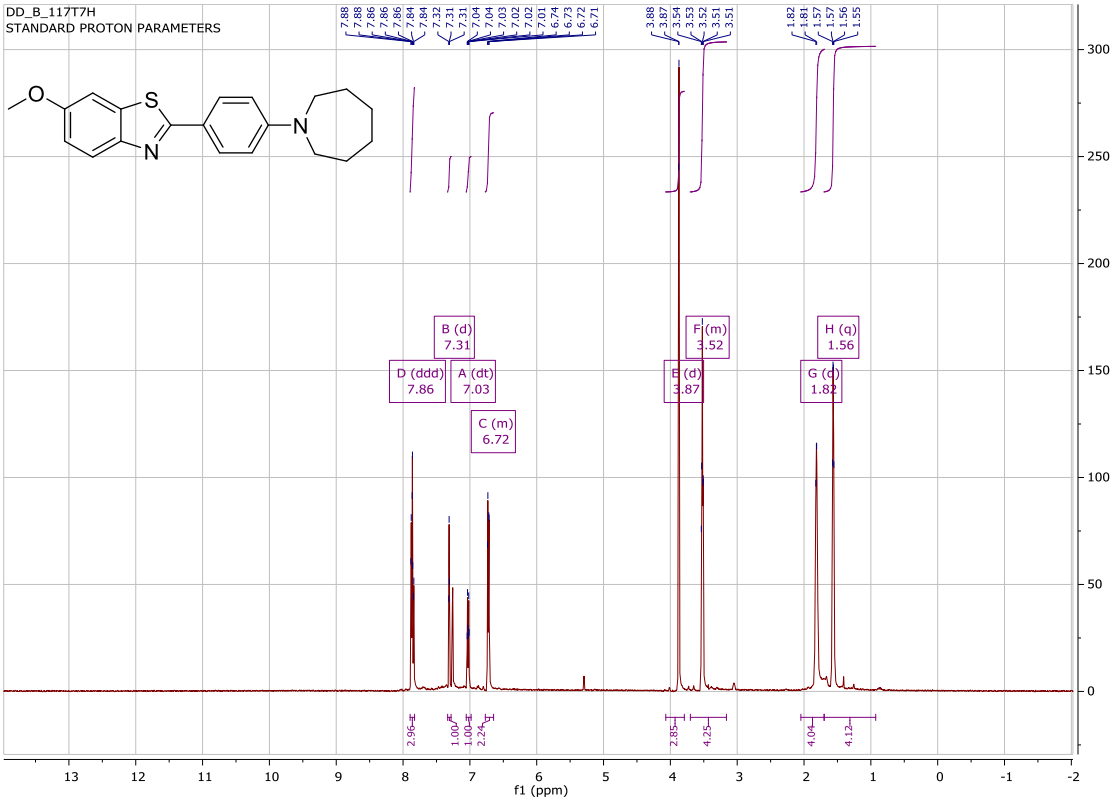

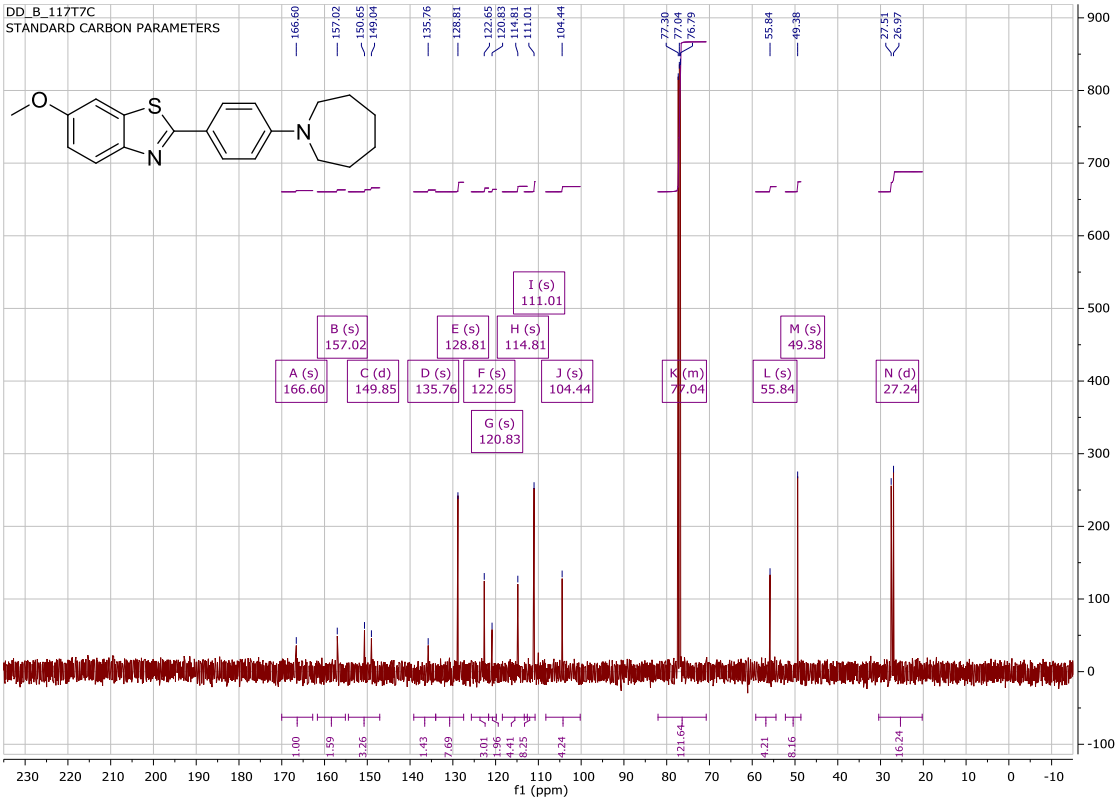

2-(4-(azocan-1-yl)phenyl)-6-methoxy-3-methylbenzo[*d*]thiazol-3-ium iodide (PAP_4)

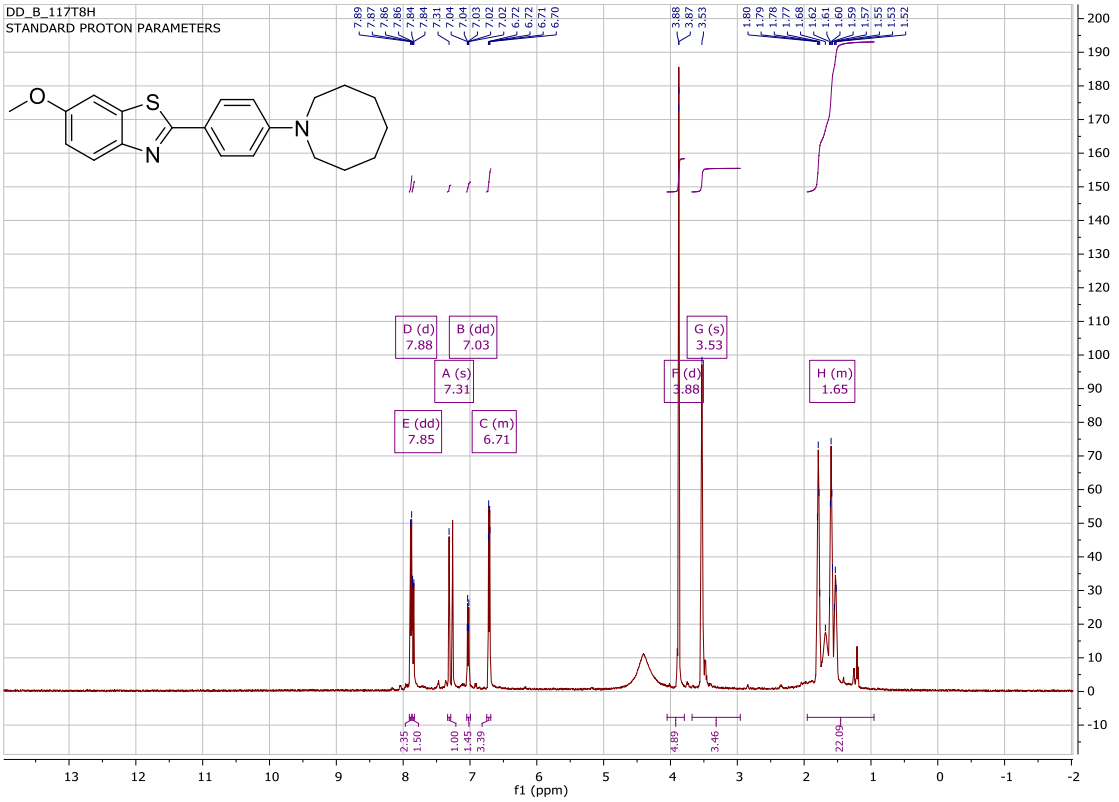

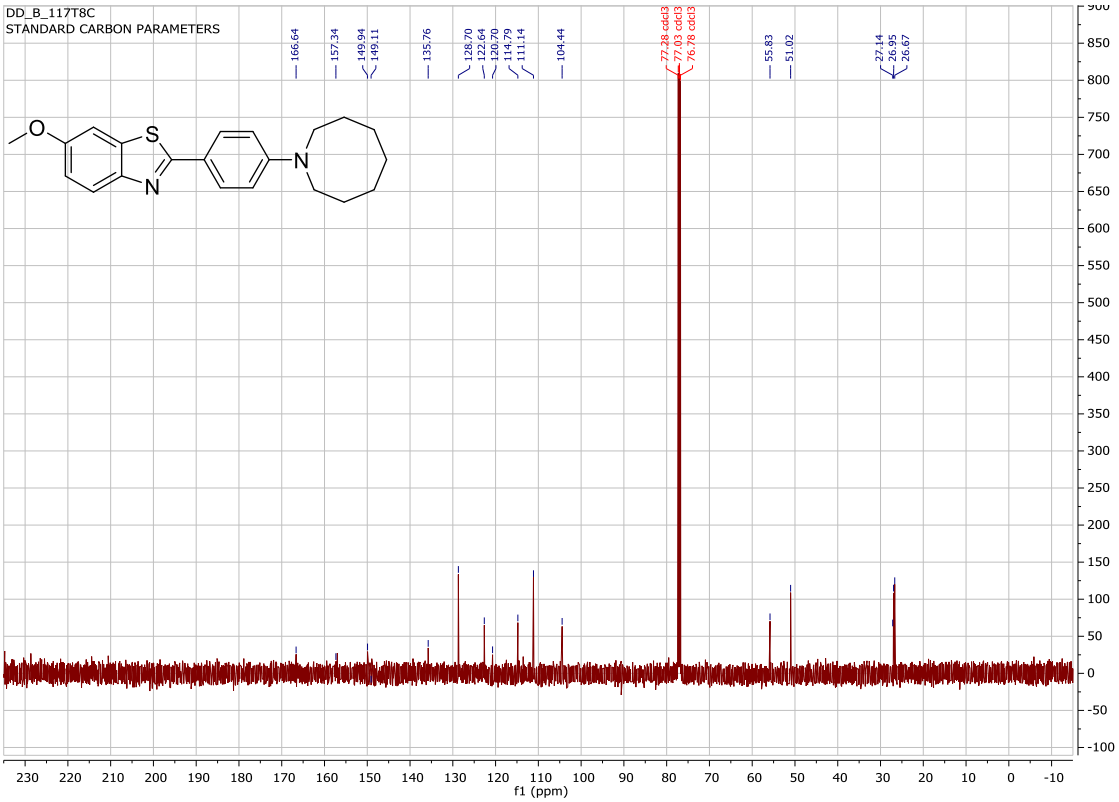

4-(6-methoxybenzo[*d*]thiazol-2-yl)-*N*,*N*-dimethylaniline (PAP_5)

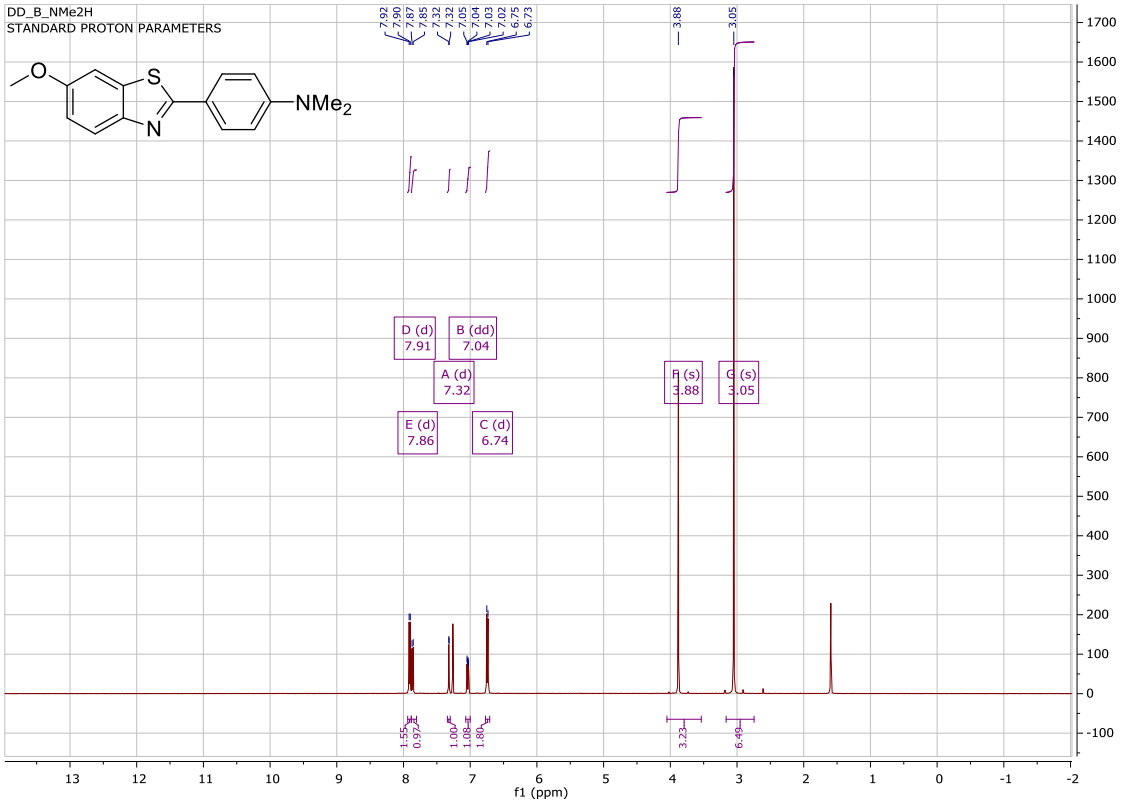

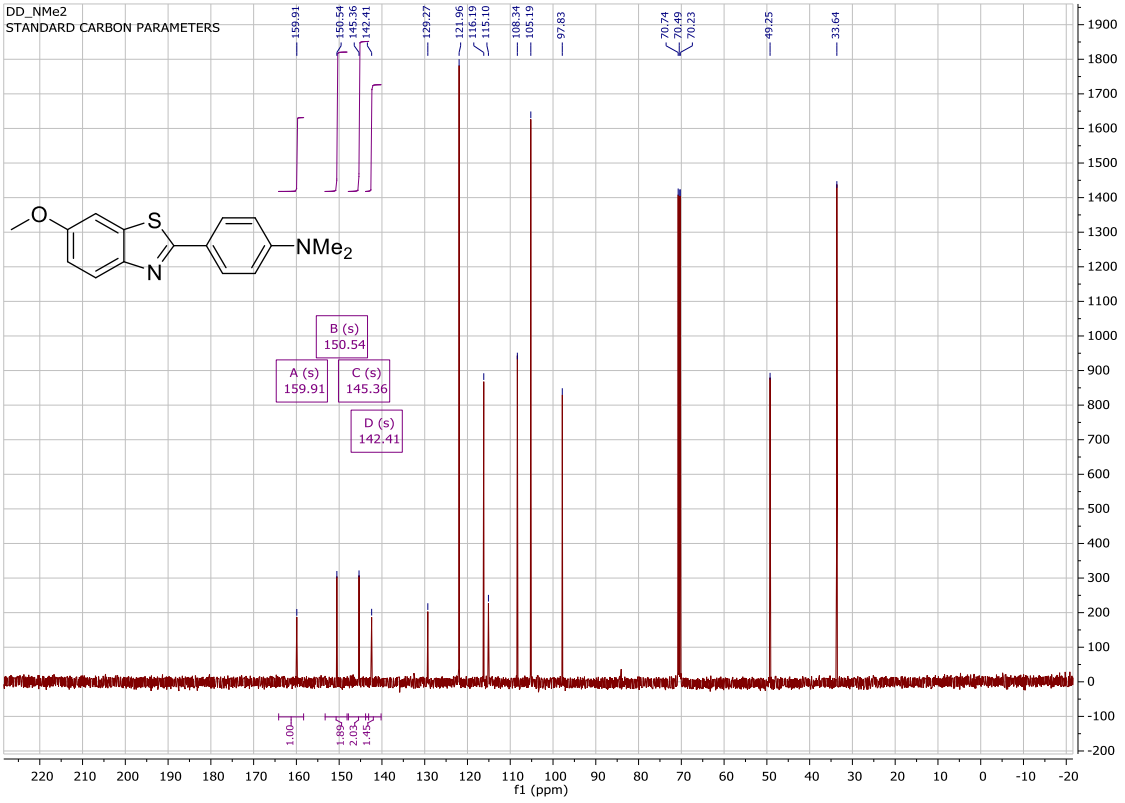

4-(4-(6-methoxybenzo[*d*]thiazol-2-yl)phenyl)morpholine (PAP_6)

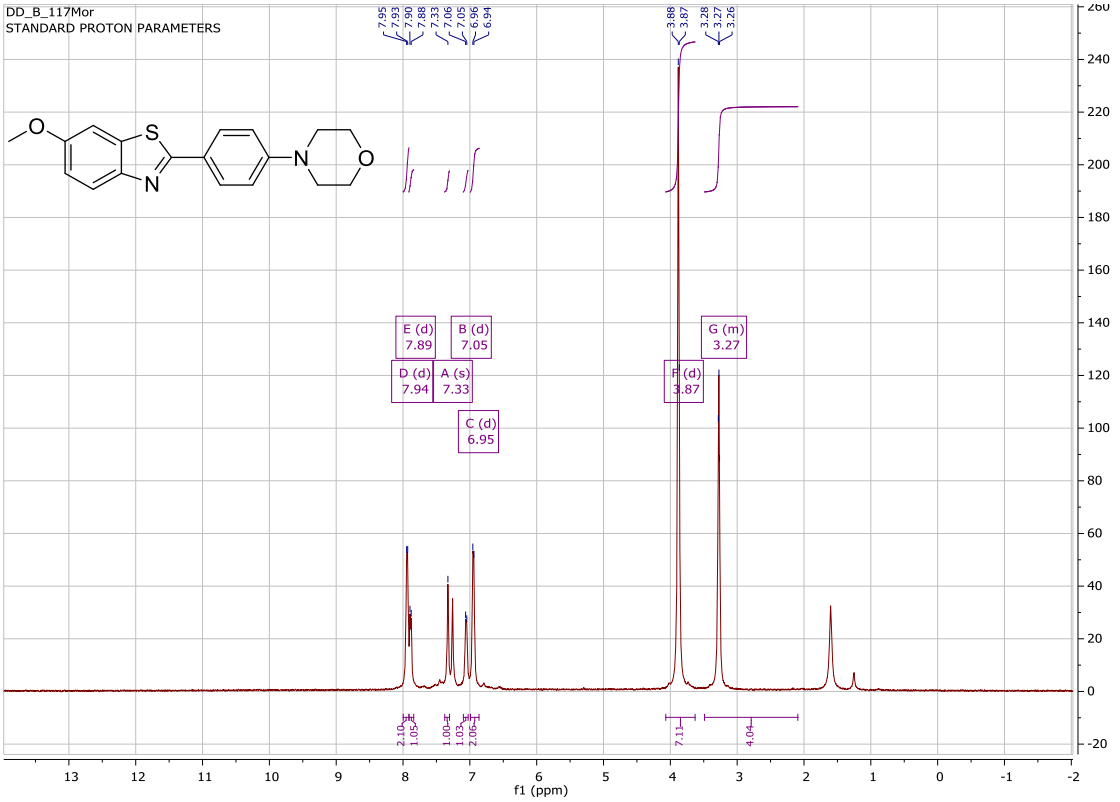

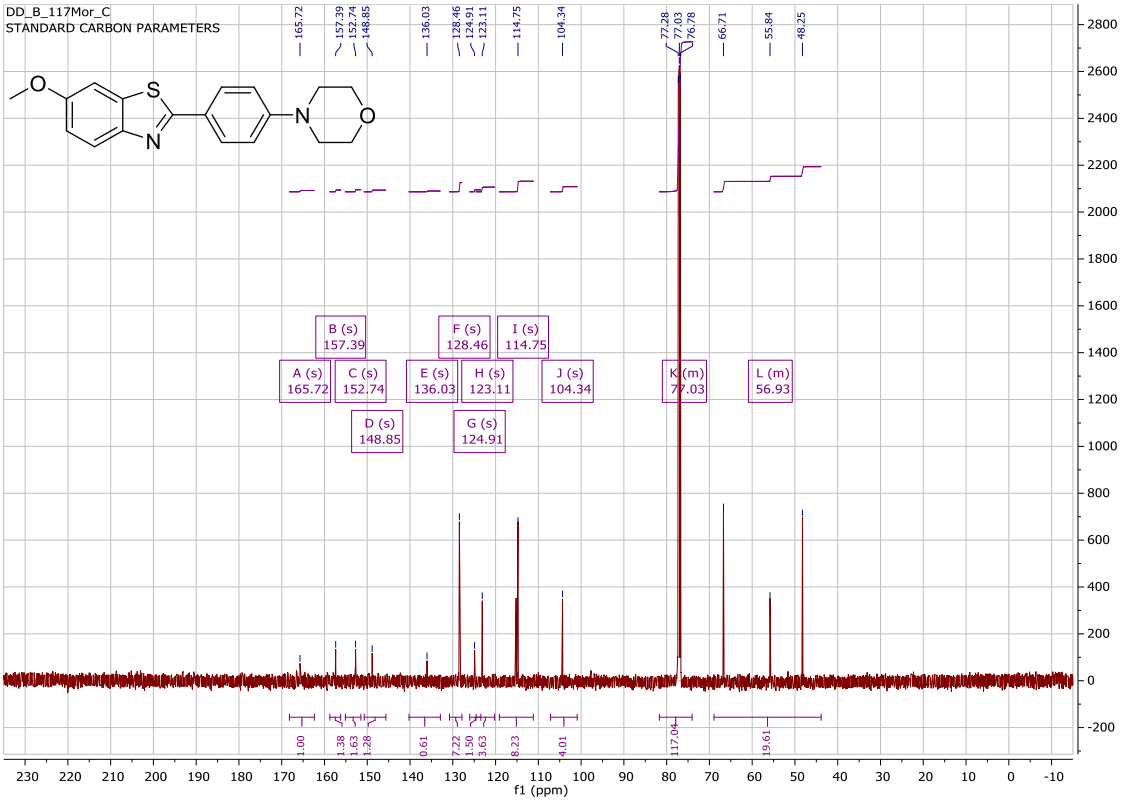

6-methoxy-3-methyl-2-(4-(pyrrolidin-1-yl)phenyl)benzo[*d*]thiazol-3-ium iodide (mPAP_1 (ThX))

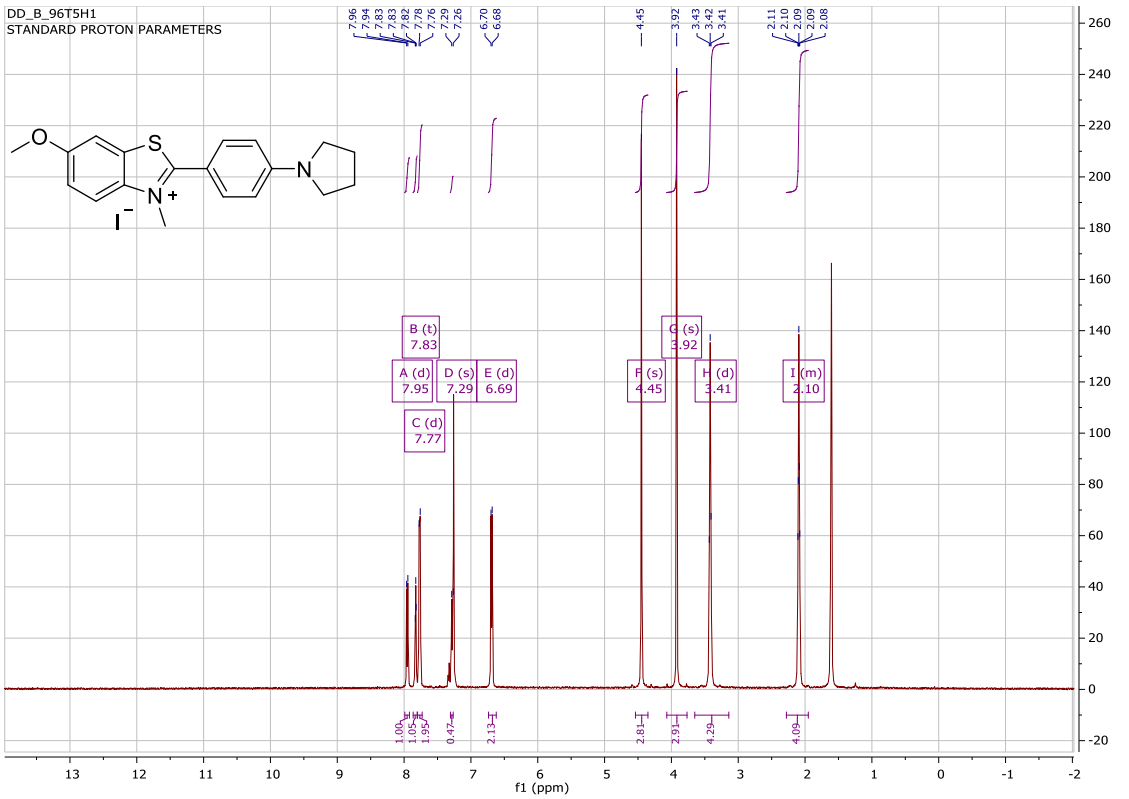

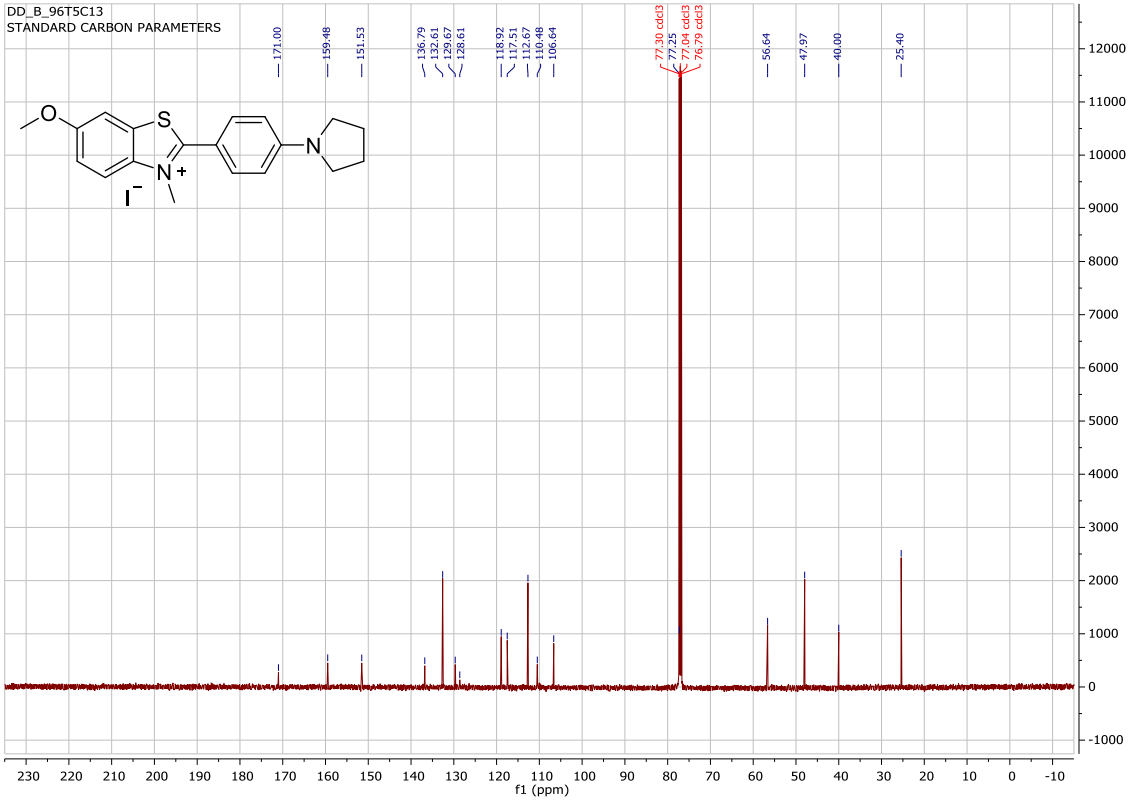

6-methoxy-3-methyl-2-(4-(piperidin-1-yl)phenyl)benzo[*d*]thiazol-3-ium iodide (mPAP_2)

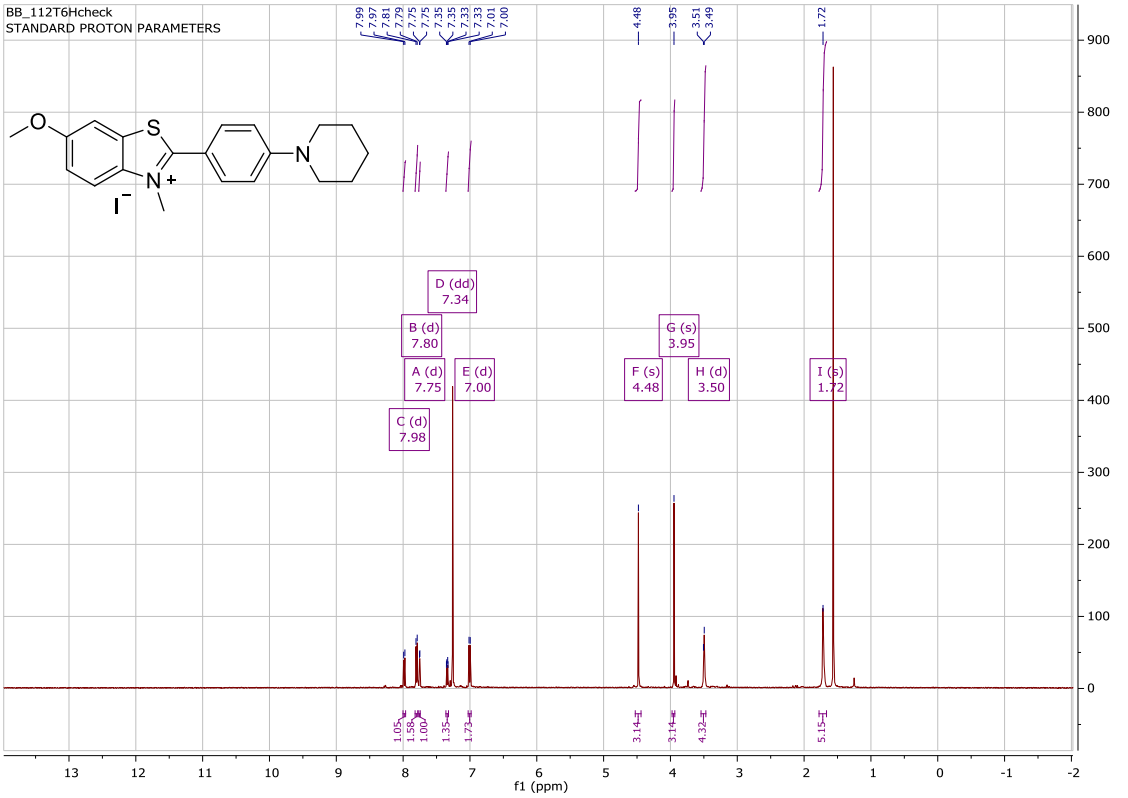

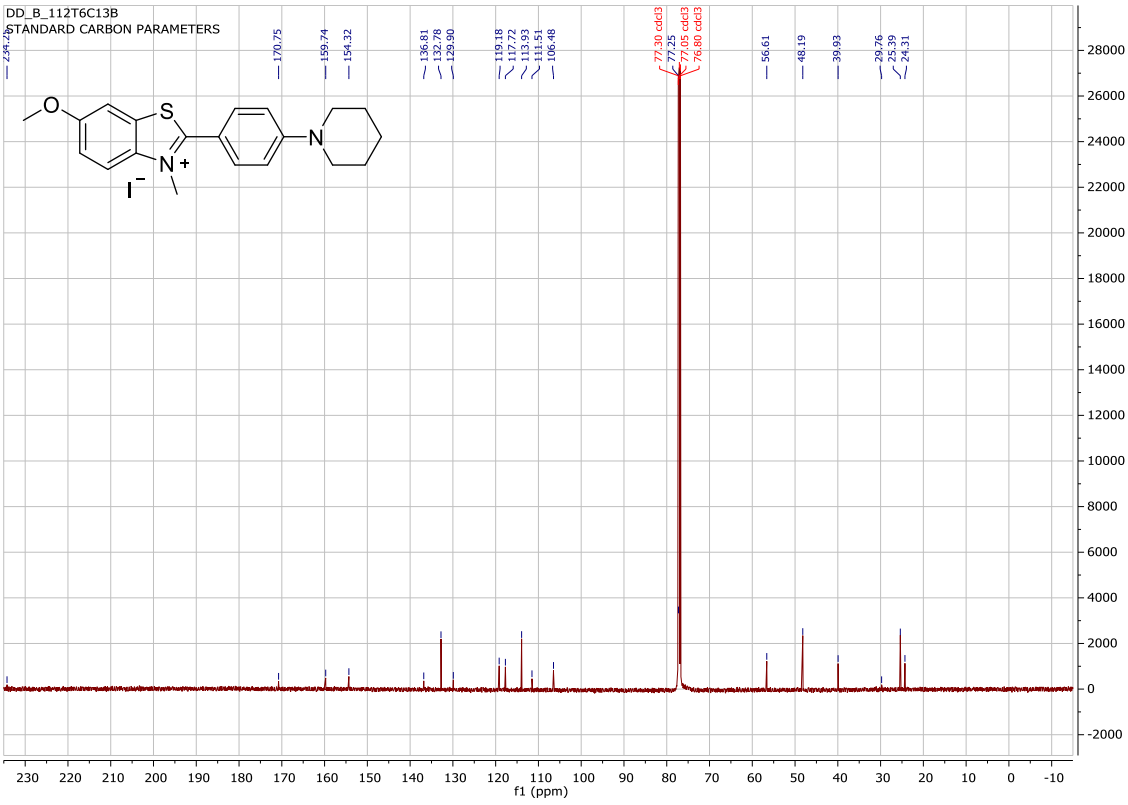

2-(4-(azepan-1-yl)phenyl)-6-methoxy-3-methylbenzo[*d*]thiazol-3-ium iodide (mPAP_3)

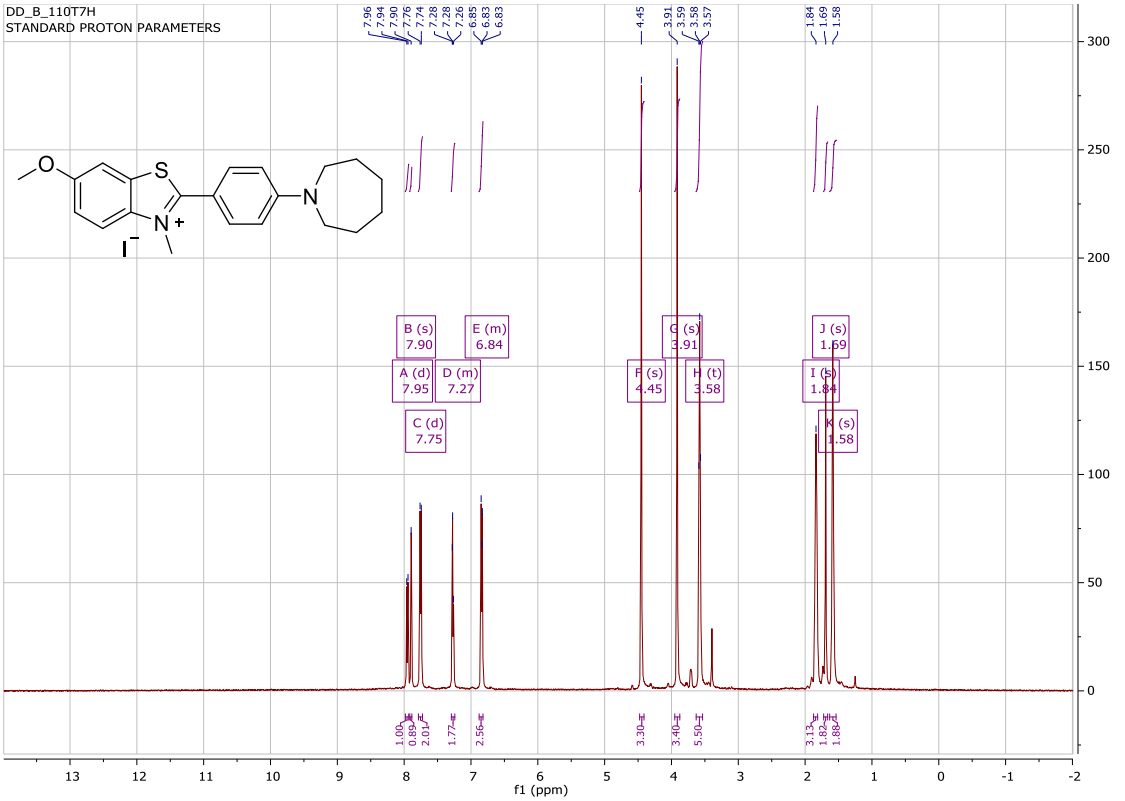

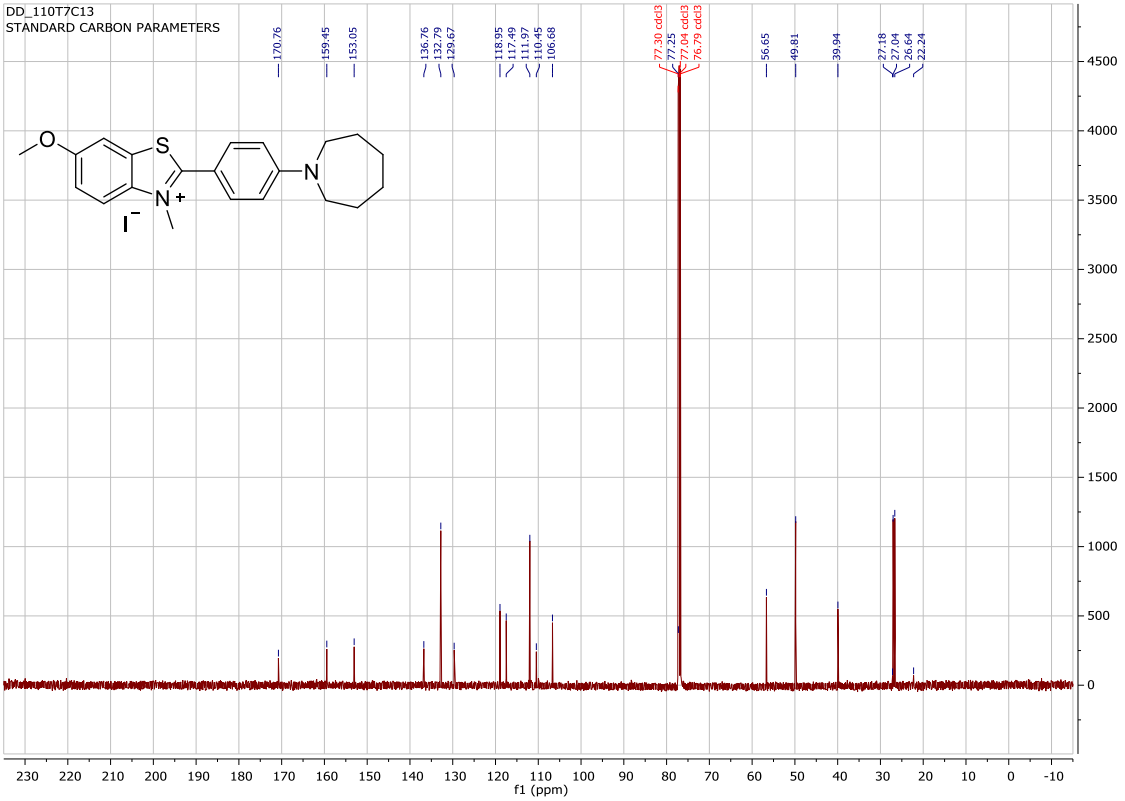

2-(4-(azocan-1-yl)phenyl)-6-methoxy-3-methylbenzo[*d*]thiazol-3-ium iodide (mPAP_4)

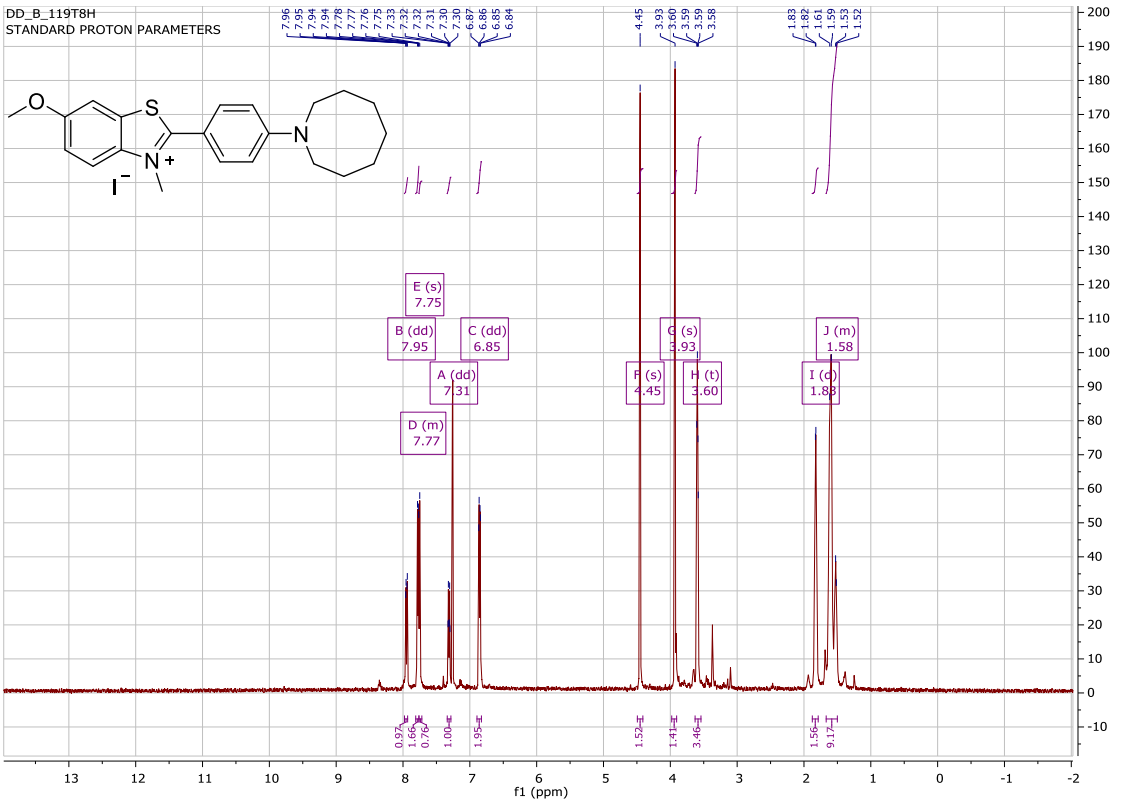

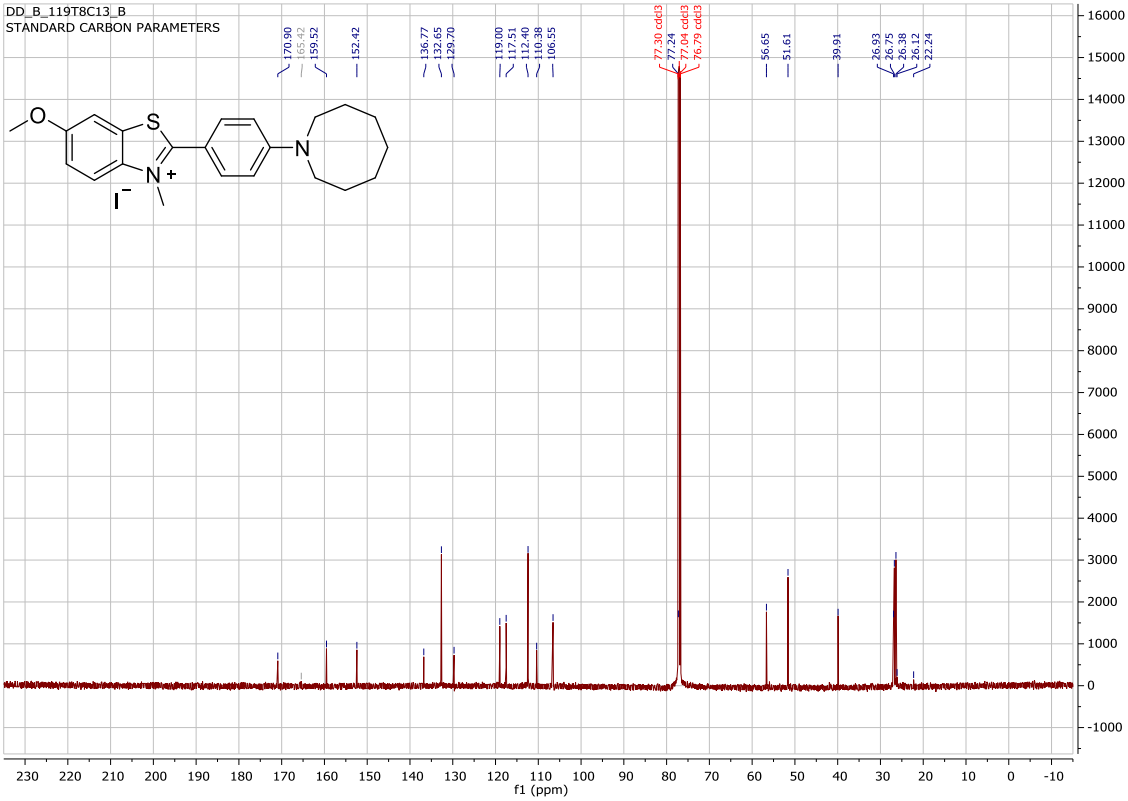

2-(4-(dimethylamino)phenyl)-6-methoxy-3-methylbenzo[*d*]thiazol-3-ium iodide (mPAP_5)

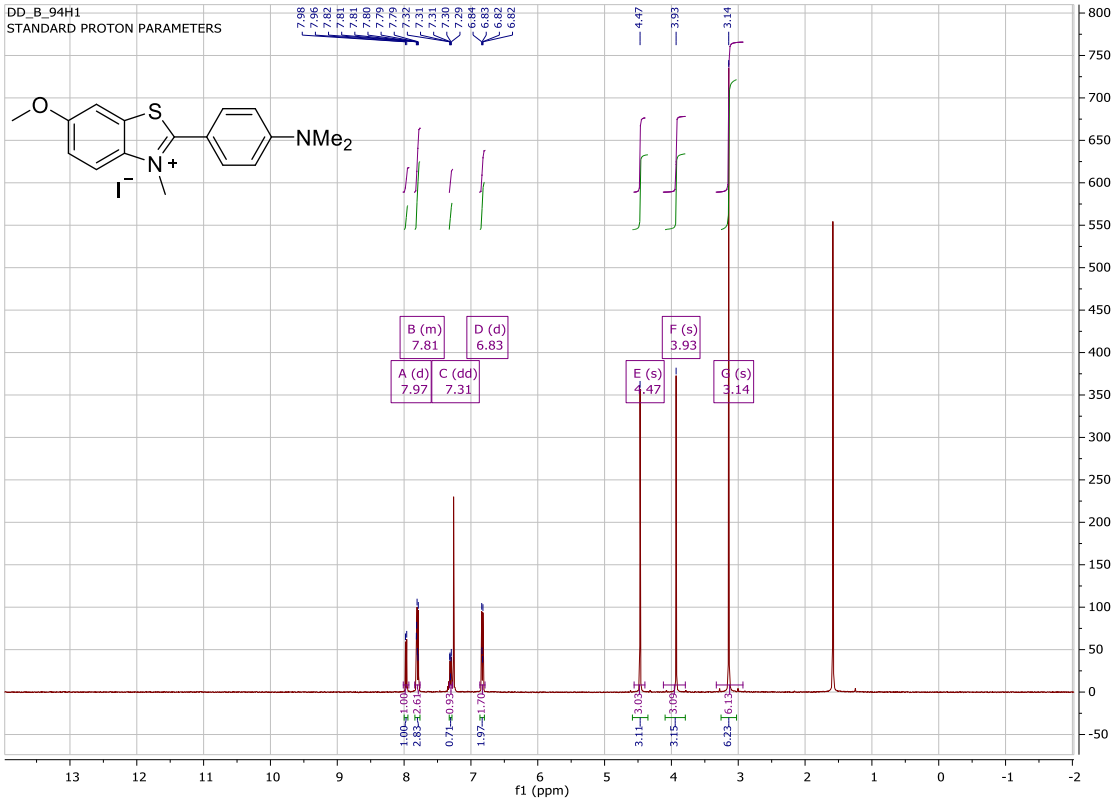

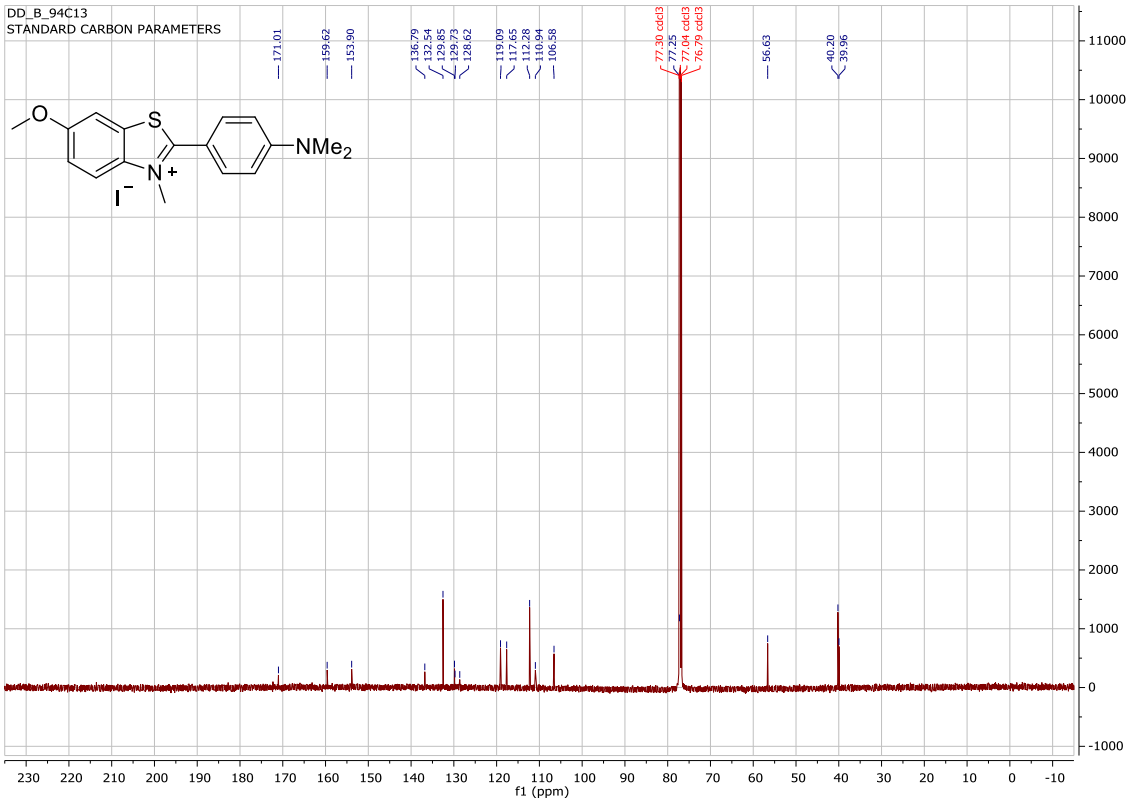

6-methoxy-3-methyl-2-(4-morpholinophenyl)benzo[*d*]thiazol-3-ium iodide (mPAP_6)

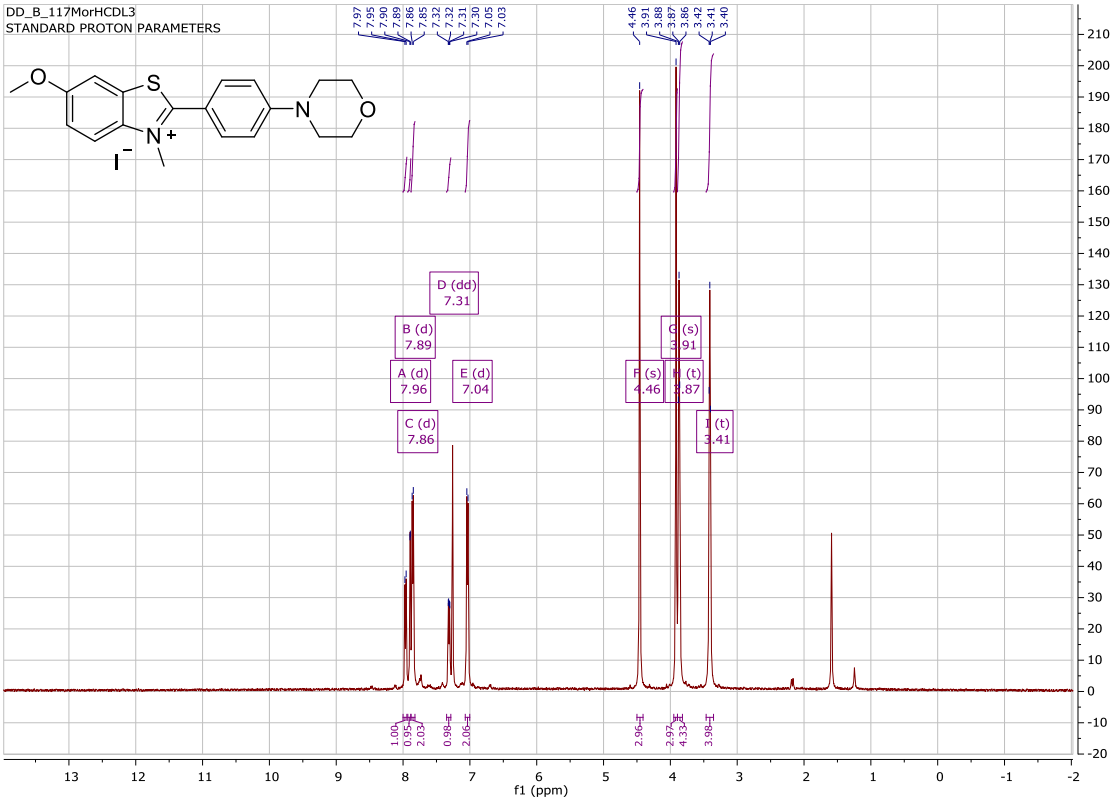

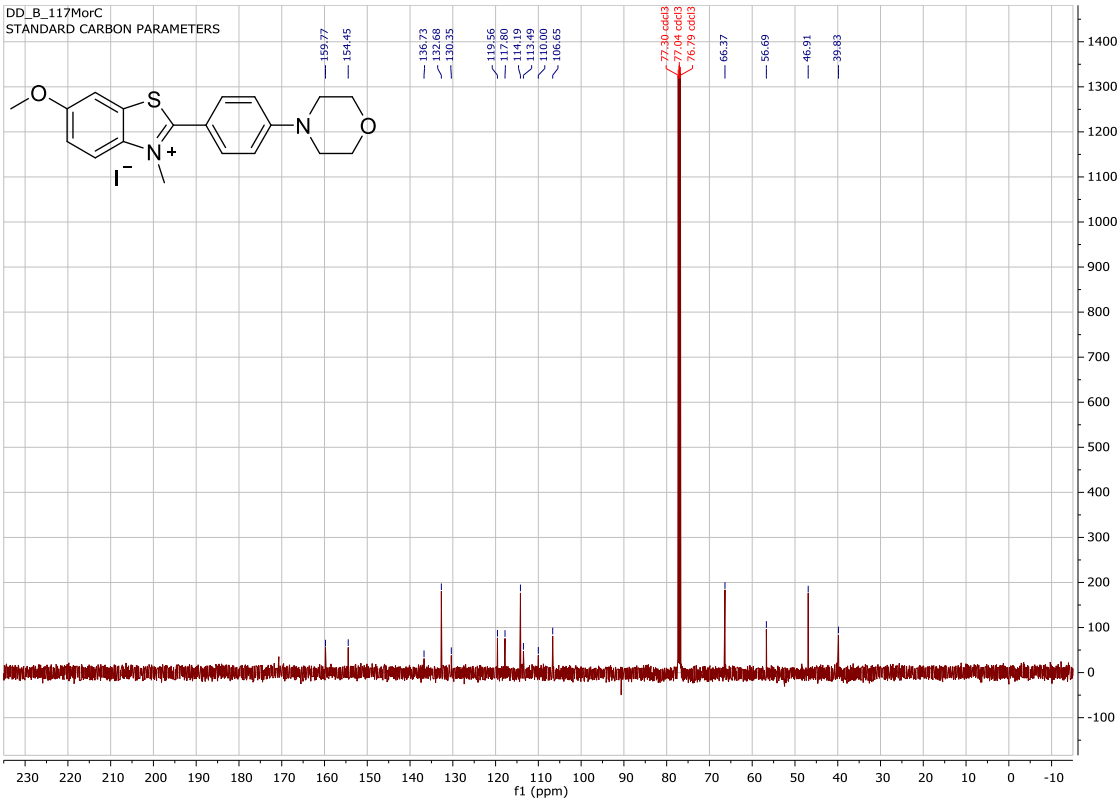

4. Supplementary References

1 D. J. Haydon, J. M. Bennett, D. Brown, I. Collins, G. Galbraith, P. Lancett, R. MacDonald, N. R. Stokes, P. K. Chauhan, J. K. Sutariya, N. Nayal, A. Srivastava, J. Beanland, R. Hall, V. Henstock, C. Noula, C. Rockley and L. Czaplewski, *J. Med. Chem.*, , DOI:10.1021/jm9016366.

2 W. Hoyer, T. Antony, D. Cherny, G. Heim, T. M. Jovin and V. Subramaniam, *J. Mol. Biol.*, 2002, **322**, 383–393.

3 A. K. Buell, C. Galvagnion, R. Gaspar, E. Sparr, M. Vendruscolo, T. P. J. Knowles, S. Linse and C. M. Dobson, *Proc. Natl. Acad. Sci.*, 2014, **111**, 7671–7676.

4 J. R. Lakowicz, *Principles of Fluorescence Spectroscopy Principles of Fluorescence Spectroscopy*, 2006.

5 A. D. Edelstein, M. A. Tsuchida, N. Amodaj, H. Pinkard, R. D. Vale and N. Stuurman, *J. Biol. Methods*, 2014, **1**, 10.